AMERICAN UNIVERSITY OF BEIRUT

# COMPARISON OF EVAPOTRANSPIRATION MEASURED FROM SURFACE RENEWAL SYSTEMS, EDDY COVARIANCE SYSTEMS, AND BOUNDARY LAYER SCINTILLOMETER OVER A POTATO FIELD IN THE BEKAA VALLEY

by
GEORGES ALBERT RAHAL

A thesis
submitted in partial fulfillment of the requirements
for the degree of Master of Science
to the Department of Agriculture
of the Faculty of Agricultural and Food Sciences
at the American University of Beirut

Beirut, Lebanon
January 2023

AMERICAN UNIVERSITY OF BEIRUT

# COMPARISON OF EVAPOTRANSPIRATION MEASURED FROM SURFACE RENEWAL SYSTEMS, EDDY COVARIANCE SYSTEMS, AND BOUNDARY LAYER SCINTILLOMETER OVER A POTATO FIELD IN THE BEKAA VALLEY

by

GEORGES ALBERT RAHAL

Approved by:

Dr. Hadi Jaafar, Associate Professor — Advisor
Department of Agriculture

Dr. Mustapha Haidar, Professor — Member of Committee
Department of Agriculture

Dr. Ali Chalak, Associate Professor — Member of Committee
Department of Agriculture

Samer Kharroubi

Digitally signed by Samer Kharroubi
DN: cn=Samer Kharroubi, o, ou, email=sk157@aub.edu.lb, c=US
Date: 2023.02.06 17:18:48 +02'00'

Dr. Samer Kharroubi, Associate Professor — Member of Committee
Department of Nutrition and Food Sciences

Date of thesis defense: January 24, 2023

# AMERICAN UNIVERSITY OF BEIRUT

## THESIS RELEASE FORM

Student Name: _____Rahal _____Georges_____Albert_____
Last First Middle

I authorize the American University of Beirut, to: (a) reproduce hard or electronic copies of my thesis; (b) include such copies in the archives and digital repositories of the University; and (c) make freely available such copies to third parties for research or educational purposes:

☐ As of the date of submission

☒ One year from the date of submission of my thesis.

☐ Two years from the date of submission of my thesis.

☐ Three years from the date of submission of my thesis.

___Georges Rahal_____ February 7, 2023_____

Signature Date

# ACKNOWLEDGEMENTS

Foremost, I would like to express my gratitude and thank my academic advisor Dr. Hadi Jaafar for his continuous help and guidance of my graduate studies and research especially for procuring all sensors and equipment of the experiment that wouldn't be possible without the GOOGLE.org grant and the Tides Foundation (Smart Irrigation using Remote Sensing and ML-Award 103808). Without his support, this thesis would not have been possible.

Besides my advisor, I would like to thank Dr. William Kustas, from the USDA, Dr. Nicolas Bambach, from the University of California- Davis, for their support and guidance during the experiment and for the wiring instructions and data processing for the Surface Renewal system.

My sincere thanks go to my committee members, Dr. Mustafa Haidar, Dr. Samer Kharroubi, and Dr. Ali Chalak for their comments, remarks and feedbacks. Additionally, I am deeply thankful to Mr. Nicolas Haddad and all AREC Staff for their assistance and support throughout the experiment and farm operations.

I thank my colleagues in the faculty of agriculture and food sciences, especially Abdul Razzak Doughan for his help during the experiment, Lara Sujud, Naji Beirouthy, Jad El Chouwani, Rim Hazimeh, Roya Mourad for their continuous help and support during my graduate studies and my thesis experiment.

Last but not least, I would like to thank my family and friends; none of this success would be possible without your efforts and support.

# ABSTRACT
# OF THE THESIS OF

Georges Albert Rahal for Master of Science
Major: Irrigation

Title: Comparison of Evapotranspiration measured from Surface Renewal Systems, Eddy Covariance Systems, and Boundary Layer Scintillometer over a Potato Field in the Bekaa Valley

An accurate estimation of the heat fluxes and evapotranspiration (ET) is important to evaluate water requirements of crops and thereby optimize irrigation management. Familiar ET sensing methods include Eddy Covariance (EC), Scintillometers and Surface Renewal (SR) systems. EC offers accurate data with low percentage of errors. Although it is non-disruptive and fully automated system that is simple to operate and maintain, the EC system has known usability of expensive sensors and energy balance closure discrepancies. Accordingly, Boundary Layer Scintillometer (BLS) and Surface Renewal (SR) are examined as alternatives to EC. In this study, the three methods mentioned above are evaluated to compare each technique's viability in determining sensible and latent heat fluxes, along with evapotranspiration and energy balance closure. The study was conducted between October and December on a semiarid irrigated potato field in the Bekaa valley, Lebanon. BLS results show good correlation with EC while comparing sensible heat flux with an $R^2 = 0.73$ and RMSE = 27.89 W/m$^2$. While analyzing SR and EC, results show better correlation between sensible heat flux with $R^2 = 0.75$ and RMSE = 21.19 W/m$^2$. The results showed closer agreement for latent heat flux and evapotranspiration, between BLS, EC and SR with BLS values only 5% greater than those from EC and 13% lower than those found using SR while EC values were 18% lower than those found using SR. Future work will need to examine the technical implementation details to maximize the advantages of adopting these alternatives to EC.

TABLE OF CONTENTS

# ILLUSTRATIONS

Figure

# TABLES

Table

# ABBREVIATIONS

| | |
|---|---|
| AUB | American University of Beirut |
| MENA | Middle East and North Africa |
| ET | Evapotranspiration |
| EC | Eddy Covariance |
| SR | Surface Renewal |
| BLS | Boundary Layer Scintillometer |
| LE | Latent Heat Flux |
| H | Sensible Heat Flux |
| G | Soil Heat Flux |
| $R_n$ | Net Radiation |
| AREC | Advancing Research Enabling Communities Center |
| $W/m^2$ | Watts per meter squared |
| R | Coefficient of Correlation |
| $R^2$ | Coefficient of Determination |
| RMSE | Root Mean Square Error |
| NSE | Nash Sutcliffe model Efficiency coefficient |
| PBIAS | Percentage Bias |
| MBE | Mean Bias Error |
| EBC | Energy Balance Closure |
| SPU | Signal Processing Unit |

# CHAPTER I

# INTRODUCTION

Much of the MENA region has suffered recently from extended, severe drought and competing need to water supply for different sectors. Municipal, industrial, environmental and agriculture have aggravated the pre-existing problem in water scarcity. The failure of water resources to meet the basic requirements of society has a host of social, economic, environmental, and political impacts (Haddadin, 2001). Agriculture is the most threatened sector by this issue. Today, in all growing regions, farmers are required to use water prudently, and introduce new technologies to manage the water resources. Thus, water management, evapotranspiration, and the exact estimation of irrigation requirement is a crucial factor for the MENA agriculture sector.

Evapotranspiration (ET) affects different ecosystem parameters and processes, such as soil moisture content, vegetation productivity, ecosystem nutrients, and water budgets (Wever et al., 2002). Generally, an increase in temperature enhances the moisture holding capacity of the atmosphere and thus, leads to an intensification of the hydrological cycle (Stagl et al., 2014). These problematic conditions are challenging agriculture and urging the sector to evolve by increasing efficiency when dealing with water. The agricultural sector in the MENA region will have to move to high-value crop production with high-resource efficiency methods and higher water productivity. This requires a shift to integrated water management concepts (Keulertz, 2019). In fact, estimating evapotranspiration is essential to know how much to irrigate, how often to irrigate, and what design of irrigation to implement. Accurate estimation of

evapotranspiration is incredibly challenging. Many methods exist to estimate evapotranspiration such as Penman monteith equation (ref-ET), Lysimeter, Surface Renewals, Scintillometer, Eddy Covariance, and Remote Sensing.

Here we compare the latent and sensible heat fluxes collected from the Eddy Covariance technique, Surface Renewal systems, and Boundary Layer Scintillometer. These three methods are among the most popular to provide such measurements with pros and cons.

Accurate measurements of energy fluxes between land and atmosphere are important for understanding and modeling climatic patterns (Yee et al., 2015). To measure turbulent surface energy fluxes, the Eddy Covariance (EC) technique has been widely used in many ecosystems such as forests (Ikawa et al., 2015), grasslands (Wever et al., 2002) and wetlands (Malone et al., 2014a; Peichl et al., 2013). Eddy Covariance is a micrometeorological method currently popular for direct observation of the exchange between ecosystem and atmosphere in terms of gas, energy, and momentum. (Liang et al., 2020). The Eddy Covariance system measures the vertical turbulent fluxes, thus the sensible and latent heat within the atmospheric boundary layers by measuring the vertical component of the wind using the three-dimensional sonic anemometer. The system is equipped with thermocouples, soil moisture sensors, soil heat flux plates to measure the soil heat flux, and a net radiometer to measure the incoming and outgoing short and long wave.

Another method to measure heat fluxes is the Boundary Layer Scintillometer. The BLS consists of a transmitter that emits a beam electromagnetic radiation that arrives to a receiver after being disturbed and scattered by air parcels and turbulent eddies in the

atmosphere. These eddies are driven by surface forcing such as wind shear from frictional drag of winds flowing over the ground, heat fluxes from the ground caused by solar incident radiation, and turbulent wakes from obstacles like plants (Stull, 1988).

The Surface Renewal (SR) method estimates the turbulent flux by measuring the instantaneous replacement of air parcels in contact with the surface between the plant canopy and the atmosphere. This measurement is done using SR's main component, which is the fine wire thermocouple that can derive the sensible heat flux. After deriving the soil heat flux and net radiation, both latent heat and ET can be calculated as a residual of the surface balance equation.

The EC and SR systems are more sophisticated than the Scintillometer. In fact, the SR requires more maintenance and skills, the EC systems are relatively expensive, labor-intensive, require well trained personnel, and provide local scale observations (Geli et al., 2019), and the scintillation methods are easier to maintain, require less data processing, provide a large-scale observation, and demand less technical skills. However, the scintillation system has its limitations as it is not as persistent in readings and fluxes can be overestimated over heterogenous surfaces (Kleissl, 2008).

Potato is one of the most cash crops planted in Lebanon and has a primary role in the Lebanese agricultural sector. All over the literature, potato water use has been well documented and studied. Application of the principle of best management practices (BMPs) for potato irrigation maximizes economic use of resources while minimizing environmental disturbances (Shock et al., 2007). The variations in water supply impact negatively on the potato shallow-rooted crop. Therefore, improving potato irrigation

management will have an impact on the productivity of this crop and will help farmers to get a better yield.

This research will introduce three methods that might help the agriculture activities in providing better quantification of irrigation water requirement, as well as decreasing the energy cost and pumping, and reducing the agriculture carbon footprint.

The objectives of this experiment are to: (1) compare sensible heat flux and latent heat flux using Surface Renewal, Eddy Covariance, and Boundary Layer Scintillometery techniques over a potato field one of the most strategic plant in Lebanon; (2) calculate the amount of water use over a late season potato field in the Bekaa Valley; and (3) understand the mode of work of sensors used to measure fluxes.

# CHAPTER II

# LITERATURE REVIEW

## A. Evaluation of Scintillometer derived fluxes

Estimates of soil sensible and latent heat flux have increasingly relied on the use of scintillometers, which are cost effective and necessitate modest maintenance (Beyrich, 2002). Rapid progress has been made in the past decades in scintillator technology with increasing use of the technique to estimate heat fluxes of vast, sometimes non-uniform, terrain (Liu et al., 2022). Scintillometry has yielded reliable flux estimates for terrains as different as "snow-covered ice, urban environs, grasslands, agricultural crops and forest canopies" (Odhiambo and Savage, 2009). Farmers favor scintillometers' ability to function at the outskirts of fields without interfering with the plantation's center (Ezzahar et al., 2007) and the tool's ability to help monitor vegetation growth and water management over areas with variable soil moistures (Geli et al., 2019). Another favorable characteristic of scintillometers is their ability to large scale obtain area average flux estimates (Asanuma and Iemoto, 2007; Evans et al., 2012; Ward, 2007). Optical scintillometers first emerged and large aperture scintillometers have had the most widespread use (Liu et al., 2022). Recently microwave scintillometers supplemented the past generations' ability to measure only sensible heat flux by combining with optical scintillometers to additionally provide latent heat flux (Liu et al., 2022). Hoedjes et al. (2002) note that scintillometers can provide areally-averaged heat fluxes with a "minimum of additional instruments (net radiometer, soil heat flux plate and anemometer." Liu et al. (2022) remark that "The data quality of the instrument depends on weather conditions, the refractive index of air, signal strength, and data post-

processing." Hu et al. additionally warn of potential disruptions from "optical interception of rainfall, insects, frost, and vertical air temperature to differentiate between the ascending and descending directions of sensible heat flux."

Changes to the refractive index of air in the infrared region are mostly caused by changes in air temperature, hence the use of infrared or near-infrared light in scintillation (Ward, 2007). Scintillometers measure fluctuations in light beam irradiance between a transmitter and receiver separated by a given height above the soil or canopy surface (Asanuma and Iemoto, 2007). The fluctuating irradiance is linked to variations in the refractive index of air caused by turbulent eddies, or atmospheric turbulence (Ezzahar et al., 2007). The instruments determine the structure parameter of the refractive index, which, when combined with roughness length – a measure of the horizontal mean wind speed near the ground – and wind speed measurements, allows the derivation of sensible heat flux using Monin-Obukhov similarity theory (MOST) (Kleissl, 2008).

The following figure from Evans et al. (2012) offers a flowchart explaining how heat fluxes can be derived from scintillometry.

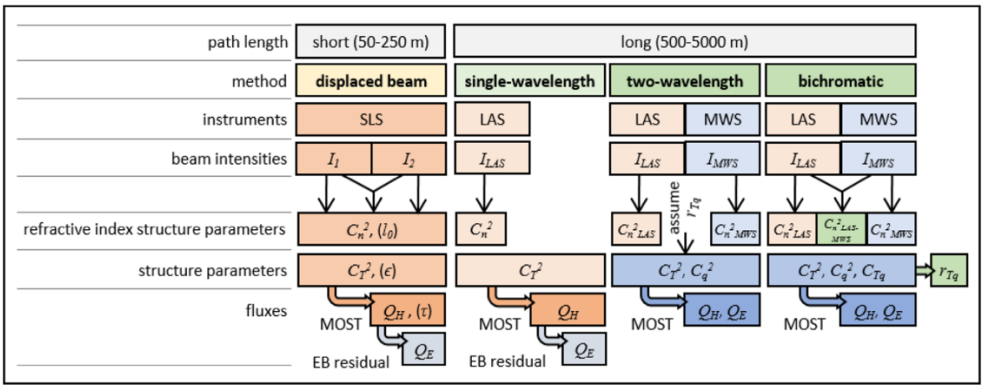


Figure 1 Methods to obtain latent (Qe) and sensible (Qh) heat fluxes using MOST (Evans et al., 2012)

Studies have demonstrated the reliability of scintillometry on uniform surfaces (Asanuma and Iemoto, 2008); heterogenous surfaces (tall and sparse vegetation) (Beyrich et al., 2002; Han et al., 2019) and "mixed agricultural landscape with complex topography that could otherwise only be obtained by aggregation of individual measurements made over each crop" (Evans et al., 2012). However, Kleissl (2008) finds that scintillometers can overestimate fluxes by a few percent over heterogenous surfaces due to the non-linearity of the structure parameters measured and the fluxes themselves. Further, Danodia et al. (2017) warn that measurements from scintillometrs require careful analysis "since poor visibility and stable stratification persisting sometimes cause substantial errors in average fluxes."

### B. Evaluation of Eddy Covariance derived fluxes

Eddy Covariance (EC) is the most widely adopted method for determining sensible and latent heat fluxes (Ward, 2017). EC has been used "from cold to tropical and from arid to humid regions," covering "water surfaces, wetlands, forests, croplands, grasslands, barelands, and urban areas" (Liu et al., 2022). The technique relies on high frequency measurements made from a several-meter high tower of wind components, temperature, water vapor and carbon dioxide spanning around areas of 100 meters (Ward, 2017). The direct estimation of water vapor exchange makes EC highly reliable (Hu et al., 2018). Furthermore, the technique does require few assumptions, omitting the need for estimates on "turbulent exchange coefficient, shape of wind profile, and buoyancy effect of air mass" (Liu et al., 2022). Nonetheless, measurements from EC are subject to "distortion produced in the sonic signal by rainfall, fog, insects, and dirt" (Hu et al., 2018). EC also requires high professional maintenance costs (Liu et al., 2022). EC is especially costly in

heterogenous surfaces and over tall sparse vegetation with high cariability of local fluxes which requires multiple systems in place (Ezzahar et al., 2007). Estimates from are also subject to error between 5% and 20% with results giving "the sum of the latent heat flux and sensible heat flux is smaller than the surface available energy" (Liu et al., 2022). Mauder at al. (2007) theorized that the gap in the energy balance is linked to "sampling errors related to inconsistent source areas for the energy balance terms; advection or storage terms not accounted for; instrument bias; and missing low or high frequency contributions." Similar reasons were proposed by Hu et al. (2018). Furthermore, adjustments and corrections in the data processing stage can lead to differences in estimates between 10 to 15 percent (Mauder et al., 2007).

Bambach et al. (2022) compared nine different methods of estimating sensible and latent heat flux from EC measurements and found that the energy imbalance (the lack of closure of the energy balance equation) led to uncertainties that "can hide issues, such as hysteresis, advection, and heat storage, which can mislead the interpretation of surface fluxes derived through the *EC* method."

### C. Evaluation of Surface Renewal derived fluxes

Surface Renewal (SR) has gained popularity in the estimation of heat fluxes for being "relatively inexpensive and easily operated" (Hu et al., 2018). SR determines the sensible heat through the temperature change rate with time obtained from high frequency measurements of air temperature, deriving latent heat from the residual energy balance equation (Hu et al., 2018). However, Kyaw et al. (1995) generalize the method for "any scalar." SR assumes a parcel of air entering a plant canopy which leads to either an increase or decrease in air temperature depending on the difference between canopy and

air temperature (Hu et al, 2018). SR results depend on the accuracy of net irradiance and soil heat flux estimates along with measurement height, wind fetch, sensor diameter, sampling frequency and choice of calibration factor (Hu et al., 2018). Andrès et al. (2020) noted calibration coefficient variations "according to meteorological conditions, with significant differences for cloudy days." Castellvi et al. (2006) were able to "automatically account for calibration coefficient changes" while keeping instrumentation simple, inexpensive and accessible and avoiding problems associated with large data sets. SR can provide accurate latent and sensible heat fluxes in rough, nonhomogeneous areas and dense canopies (Hu et al., 2018; Castellvi et al., 2006) but less reliabale estimates in high humidity conditions and apparatus is sensitive to damage in high wind conditions (Hu et al., 2018). SR has been reliably used on terrains and crops such as "bare soil, open water irrigated pasture (tall fescue), sugarcane, flood-irrigation pecan, rice, lagoon, grapevine, sorghum, wheat, grass, vineyard, tomato" (Hu et al., 2018). Hu et al. (2018) additionally note that the reliability of estimates from SR are linked to the accuracy of net irradiance and soil heat flux. Gray et al. (2021) attempted to overcome the dependency of established SR methods on EC for calibration with good results, allowing "novel deployments such as low-cost, continuous monitoring and on moving platforms."

### D. Intercomparison between Scintillometer, Eddy Covariance, and Surface Renewal fluxes

Kang and Cho (2021) conducted a review of heat flux estimation in Asia noting that most experiments comparing scintillometers and EC were "conducted in large areas displaying landscape heterogeneity" where discrepancies were found between the two methods while "measurements agreed well over homogeneous surfaces." Two studies each over a

period of one month on a homogeneous, irrigated pasture found “excellent agreement” between EC and scintillometer estimates of sensible heat flux.

Odhiambo and Savage (2009) found that EC, Scintillometers and SR sensible heat results were mostly in agreement “especially on cloudless days” for a study of a mixed grassland in which data was collected for over two years.

Castellvì et al. (2006) found that for a field of sprinkler irrigated rice planted in a flat, windy and semiarid site within the Ebro River basin, Spain, sensible heat estimates from Surface Renewal were highly correlated (0.77) to estimates obtained from EC under stable conditions while unstable conditions resulted in excellent correlation (0.94). Moreover, SR led to “good energy balance closure that was superior to that obtained using the Eddy Covariance method,” overcoming one of the main deficiencies of the EC method.

Pozníková et al. (2018) studied a wheat plantation grown on black earth soil in the Czech Republic with a maximum crop height of one meter in rectangular a field with a length of 800 m and width of 325 m with an open path EC system elevated at 2.7 meters sampling at 10Hz and scintillometer diameter of 0.15 meters at the same height as the EC system over 75 days (four periods from green wheat, mature wheat, then post-harvest when soil is dry then wet). The two methods agreed only for the green wheat period while scintillometry overestimated sensible heat for the remainder of the studied period. Scintillometers also overestimated latent heat for the entirety of the studied period. The researchers noted that similar studies found underestimations of sensible heat using EC under heterogeneous conditions. The researchers also evaluated Surface Renewal using eight thermocouples with wire diameters between 13 and 75 micrometers at a 10 Hz

sampling frequency which showed weaker result than either of EC or scintillometers, except when latent heat was evaluated over longer time scales.

Parry et al. (2019) studying a vineyard in California found good correlations between latent heat estimates given by EC, scintillometry and a novel stand-alone SR system that did not require calibration with EC which was also capable of responding to micrometeorological changes in the studied area's conditions. The researchers concluded that the "new SR method could potentially be used as a low-cost tool to provide growers with field-specific estimates of crop water use and stress for irrigation management in vineyards" (Parry et al., 2019). Earlier attempts at using SR over a vineyard yielded low correlation (0.56) with EC (Hu et al., 2018), demonstrating the rapid advances being made in SR technology and their potential.

Wang et al. (2021) found that SR could provide an economical alternative to EC after a comparison of the techniques on a tea plantation in China showed respectively high (0.80) and very high (0.93) correlations for sensible heat and latent heat fluxes between the two methods. Hu et al. (2018) found that "the SR method inexpensively demonstrates performance efficiency under different climatic conditions and surfaces as compared to the EC method" after reviewing several experiments out of which eight studies had flux measurements correlations greater than 0.9; three over 0.8 and only three with lower values.

### E. Advantages and Disadvantages of Scintillometer, Eddy Covariance, and Surface Renewal

Allen et al. (2011) noted that scintillometers are distinguished by their "ability to derive sensible heat flux that is integrated over a long transect, up to several km in length" in

addition to straightforward operation and maintenance and consistent results. Weaknesses noted by the same researchers include financial cost, inability to measure direction of sensible heat flux, derivation of latent heat from energy balance residual and the need to estimate friction velocity.

EC which many researchers consider the status quo for energy flux measurements can directly measure the latent energy, its use of continuous, direct sampling and the automated nature of its components (Allen et al., 2011). EC also carries a number of disadvantages including elevated energy balance closure error, fragile and expensive instruments which require highly skilled operators and the need for post measurement "corrections" (Allen et al., 2011). Odhiambo and Savage (2009) compare the need for corrections in EC "for flow distortion and coordinate rotation are applied" to scintillometers which only need "a correction for water vapour pressure."

SR is distinguished by its low financial cost and ease of operation, its reliability on heterogeneous terrain, its reduced fetch requirement, its ability to provide flux estimates without wind speed, and the ease of calculations which allows "repetition of results inexpensively" (Hu et al., 2018). However, SR is error prone during high humidity conditions and instruments can be damaged in high wind conditions (Hu et al., 2018). Furthermore, SR can experience periods of intermittent sampling where no measurements are recorded (Gray et al., 2021).

### F. Potato Plantation

Potato is one of the most strategic crops in the world in Lebanon and especially in the Bekaa valley. Potato is one of the most important food crops in the world after wheat,

maize, and rice with a production of around 311 million tons from 19 million hectares of land in 2003 (Vreugdenhil et al.). Therefore, finding solutions for water management over potato fields will have an impact on the whole water management in the country. Potato requires a warm soil temperature and a growing season that ranges between 120 and 150 days depending in the weather conditions

# CHAPTER III

# MATERIALS AND METHODS

This experiment was conducted in a potato field at the premises of the American University of Beirut's Advancing Research Enabling Communities Center "AREC", between August 2021 and December 2021. This chapter will explain the procedures carried out in this experiment.

## A. Site Description

The experiment was conducted on an 18 dunum potato field in the Bekaa valley at the American University of Beirut's farm: AREC – Advancing Research Enabling Communities Center (33°55'16.33 N – 36°04'29.01'' E). The location of the center is in the MENA region and is known by its semiarid climate with cold winters and dry hot summers. The site is flat with no slope with an elevation of 995 meters above sea level. The average annual precipitation is 520 mm with a coefficient of variation of 0.31. (Jaafar, et al., 2017)

Figure 2 Potato field – study area

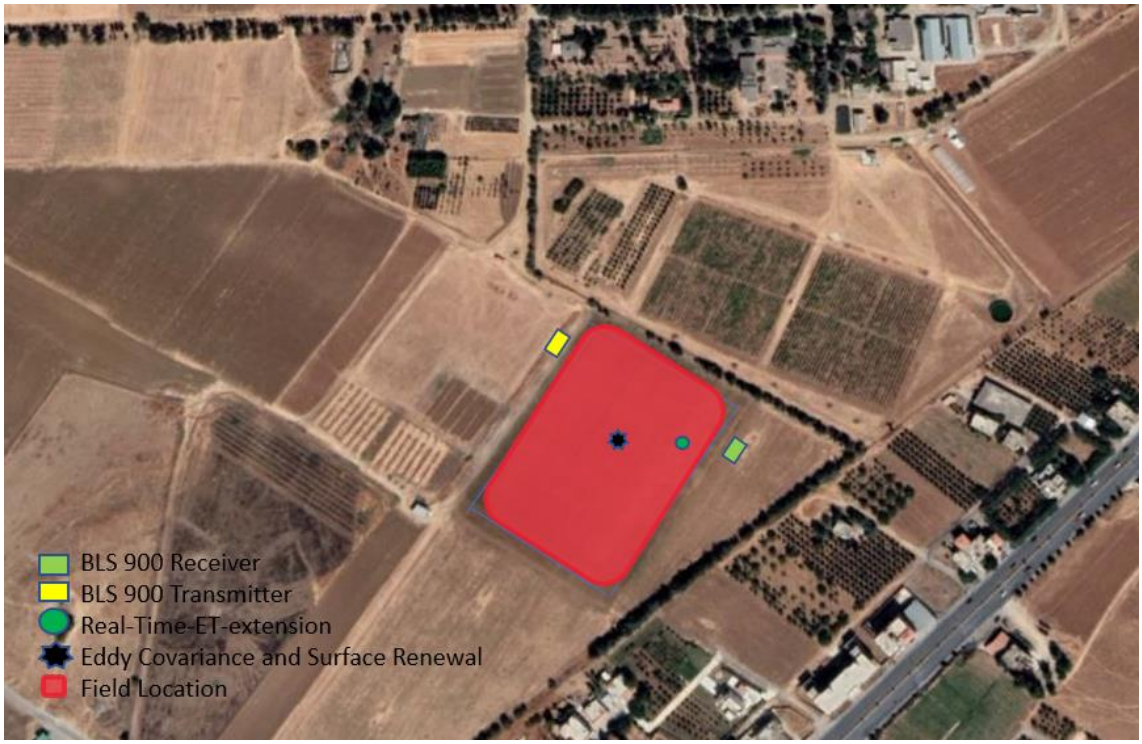

Figure 3 Location of the BLS 900 EC SR in the potato field

**B. Potato Plantation and Irrigation**

- **Land Preparation**

Land was ploughed using a moldboard and disk plough as primary tillage and a disk harrow as secondary tillage to aerate the topsoil, mix the soil surface, and destroy clods. On august 6$^{th}$, the land was irrigated with an irrigation depth of 64 mm before 4 days of planting. Five tons of Akkari Agria potato tubers were soaked in fungicide (Fosetyl-Aluminum) and gibberellic acid for 1 minutes and let dry for 1 day. Tubers were subsequently planted in the late growing season (8 August 2021) in a 1.8 hectares' field (18 dunums). The spacing within potato tubers was around 30 cm, and the inter row spacing was 75 cm. Tubers were planted at a 25 cm depth. During plantation, fertilizers were added at a rate of 50 kg of DAP + 25 Kg of granular grade 15 nitrogen – 15 phosphorus – 15 potassium with trace elements per dunum.

- **Irrigation System**

The irrigation of the site was divided into two phases:

Phase 1:

Irrigation was applied every 7 days starting August 23rd till September 20th. A sprinkler irrigation system was installed at a spacing of 12 x 18 m, at a pressure of 3.6 bars. A total amount of 48 mm of water was applied using sprinkler with flow of 1.83 $m^3$/hr.

Phase 2:

Irrigation was applied every 7 days starting October 1st till November 10th using micro sprinklers of 130 liters per hour flow at a 2.5 bar pressure, with a main pipe diameter of 90 mm, a sub main of 75 mm, and a lateral of 32 mm. Fifteen micro-sprinklers were installed in each lateral. The micro-sprinkler system was installed at a spacing of 5 x 5 m which offers an irrigation overlap. The total irrigation depth per irrigation was of 30 mm. Two pressure gauges were installed one near the valve and one at the end of the last lateral to monitor the amount of water irrigated and its uniformity.

Two flow meters and a rain gauge were installed in a way to represent the field to measure and monitor the irrigation depth. The total irrigation depth recorded by the rain gauge was 191 mm (41 mm of rainfall and 150 mm of irrigation)

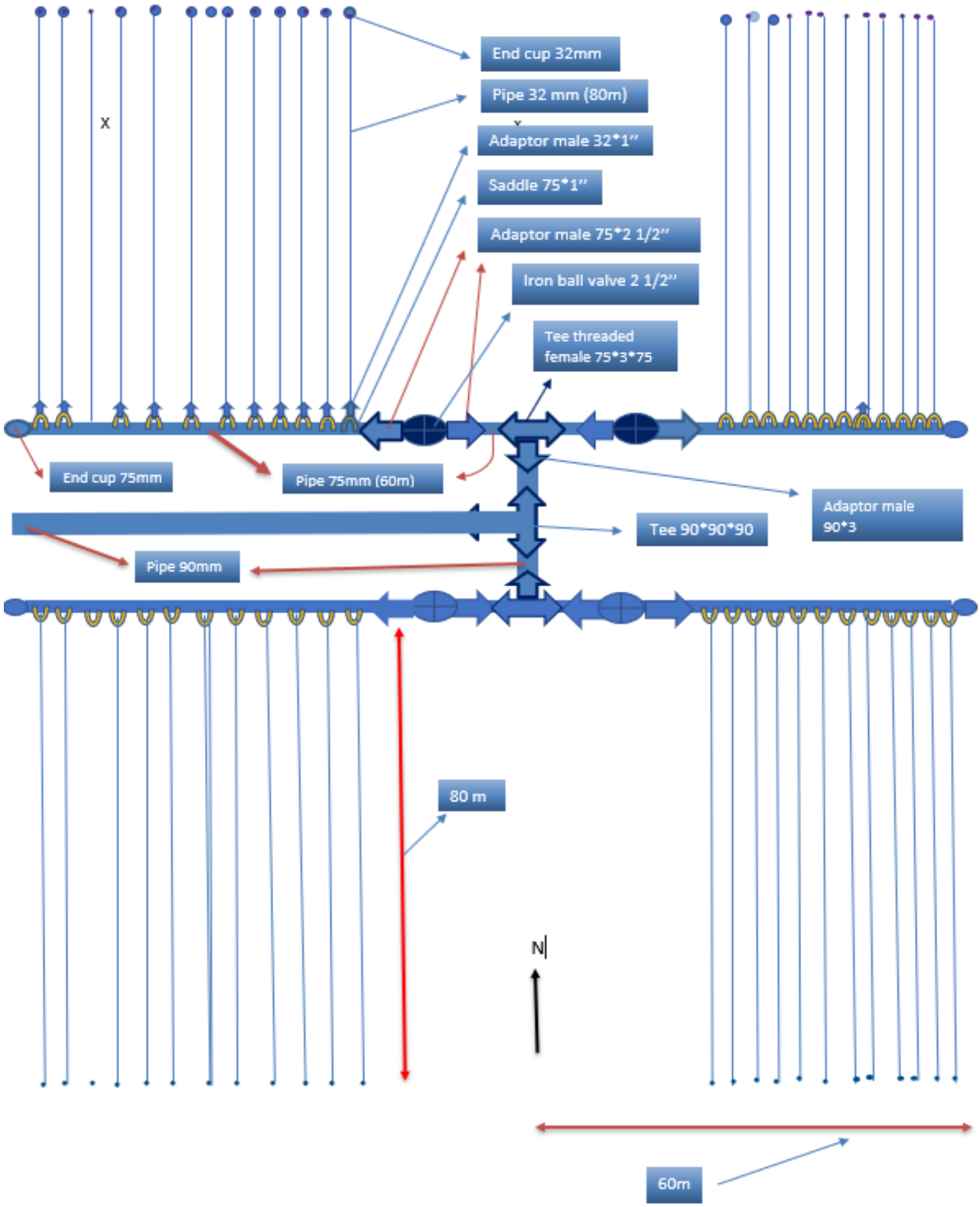


Figure 4 Micro-sprinkler irrigation design

- **Agricultural Practices**

To eliminate weeds, the entire experimental areas received a standard application of metribuzin (Sencor$^{R}$, 70%, PE) at 0.75 kg ai.ha$^{-1}$ two weeks after potato sowing with a boom sprayer at a rate of 400 L.ha$^{-1}$.

On September 21$^{st}$, Urea was applied during hilling the potatoes in bands 40 days after planting at a rate of 300 Kg. ha$^{-1}$ to add more soil and organic matter around the tuber, keep weeds down around the root zone, and encourage tubers to grow. 50 grams per 20 liters of chlorothalonil, 6 grams per 20 liters of acetamiprid, and 8 grams per 20 liters of lambda-cyhalothrin was applied to protect the plants from fungi, bacteria, nematodes, and insects.

The harvest day was on December 3$^{rd}$. 31 tons/1.8 ha of first grade quality potato along with 16 tons/1.8 ha of second grade quality potato was harvested and sold on the market.

**C. Flux measurements**

- **Eddy Covariance Measurement**

The Eddy Covariance technique is an open path system manufactured by Campbell scientific company which is a leading designer and manufacturer of data loggers and sensors related to weather, water, energy, gas, flux, and soil. Since the Eddy Covariance system requires continuous power supply, a 2.5-meter-tall tripod tower powered by two solar panels and a lithium battery was implemented in the potato field containing an IRGASON 3D sonic anemometer and a temperate and relative humidity probe. The Irgason derives water vapor, carbon dioxide, fluctuations on the wind velocity component and temperature, latent, and sensible heat fluxes by measuring the vertical turbulent fluxes within the atmospheric boundary layers. The sonic anemometer was placed at 2

meters above the canopy and mounted to an EC 100 data logger. Moreover, air temperature and humidity were measured using a hygroview temperature and relative humidity sensor placed at 2.3 meters above canopy. The incident and emitter shortwave and long wave radiation was measured using a four-way net radiometer placed at 2.5 meters above the potato canopy. Furthermore, soil temperature, moisture, water content, and heat fluxes were recorded using three soil thermocouples (TCAV) placed horizontally at a depth of 2, 4, and 6 cm, three water content reflectometer (CS655) installed horizontally at a depth of 3 to 15 cm, and three soil heat flux plates placed at 8 cm soil depth. These sensors were all mounted, connected, and stored in a CR1000X data logger at a 30 minutes averaging period. The data logger was installed in an enclosure at the base of the tripod. The latter contained a CR1000X data logger, a granite volt 116, and a terminal block connected to the power supply tripod enclosure containing the battery, the Morningstar sunsaver-10 regulator connected to the solar panels. The data collected from the Eddy Covariance was retrieved using a flash card which can be replaced after transmitting the data to a computer and processed using a software "PC 400" to retrieve the data.

The Eddy Covariance tower was implemented on October 12, 2021 and was programed to record half hourly data.

- **Eddy Covariance Data Processing**

The Eddy Covariance measures the covariance between fluctuation of vertical wind velocity and fluctuation of temperature then compute the sensible heat flux. It also measures the latent heat of vaporization and the covariance of the water vapor density and vertical wind speed to derive the Latent heat.

It uses the following formulas:

$$H = \rho\, Cp\, w'\overline{Ts'} \quad (1)$$

$$LE = \lambda\overline{w'q'} \quad (2)$$

Where H is the sensible heat flux, ρ is the air density, Cp is the specific heat of air in J/g/K, W is the vertical wind speed in m/s, T is the air temperature in K, LE is the latent heat flux, $\lambda$ is the latent heat of vaporization in J/g, and q is the water capor density in Kg/m3. The overbar over the covariance is both formulas that indicate the averaging of time.

Fully corrected data was collected since the Easyflux which is a CRBasic program that enables the data logger to assemble fully corrected data was installed on the EC CR 1000X. Therefore, sensible heat Flux (H), Latent heat flux (LE), net radiation ($R_n$), and ground heat flux (G) can be calculated using the open path Eddy Covariance system installed along energy balance sensors.

- **Surface Renewal Measurement**

The Surface Renewal system which is also manufactured by Campbell Scientific and the Eddy Covariance technique was installed on the same tripod powered using the same solar panels and battery. Both techniques were connected to the data logger (CR1000X) and a granite volt 116. The system contains a type E fine wire thermocouple (FW3) installed at a height of 2 meters to measure high frequency air temperature, thus the sensible heat flux. Two Apogee infrared radiometers (IRR) (one SIF-121 and one SIF 1H1) were installed at 2.5 meters above the canopy to measure the temperature of the pant cover.

- **Surface Renewal Data Processing**

The sensible heat flux is derived using the formula:

$H = \alpha \times z \times \rho \times Cp \left(\frac{a}{d+s}\right)$

Where z is the thermocouple height above the soil (m), ρ is the air density ($g/m^3$), Cp is the specific heat of air at constant pressure (J/g/K), a is the average ramp amplitude (K), d is the duration of the air parcel heating, s is the quiescent period that follows the sweep phase of the air parcel (s), (d+s) are collectively called the mean ramp period (s) and α is the calibration factor obtained from the slope of the least square regression between $H_{EC}$ vs uncalibrated $H_{SR}$ forced through the origin.

The ramp amplitude (a) and the duration (d+s) are calculated using the Van Atta ramp model (1977).

$S^n(r) = \frac{1}{m-j} \sum_{i=1+j}^{m} (T_i - T_{i-j})^n$

where m is the number of data points in the 30-min interval measured at frequency (f), n is the order of the structure function, j is a sample lag between data points corresponding to a time lag (r = j/f), and $T_i$ is the $i^{th}$ temperature sample (K).

The mean amplitude (a) during the time interval of experiment is determined by solving the real roots in the following equation:

$a^3 + pa + q = 0$

Where

$p = 10S^2(r) - \frac{S^5(r)}{S^3(r)}$

And

$q = 10S^3(r)$

While the mean ramp period was calculated as the following:

$$d + s = -\frac{a^3 r}{S^3 r}$$

After measuring the sensible heat, latent heat can be derived from the energy balance equation: Latent heat = Net radiation – the sensible heat – the ground heat

Using the data collected from the four-way net radiometer, the net radiation ($R_n$) received at the surface can be calculated $R_n$ = (short wave in + long wave in) – (short wave out + long wave out), and the ground heat flux can be calculated using the data collected from the three soil thermocouples, the three soil moisture sensors, and the three soil heat flux plates.

Figure 5 Eddy Covariance and Surface Renewal Systems in the Potato Field

- **Boundary Layer Scintillometer Measurement**

The BLS 900 Scintillometer installed in the potato field contains two transmitters tangent to each other and one receiver with a diameter of 0.15 meters and operates at a wavelength of 800 nm. This Scintillometer is manufactured by Scintec. The transmitter and receiver were placed on tripods with a path height of 2 meters and a path length of 150 meters.

The receiver was connected to the Signal Processing Unit (SPU) which is also connected to a so-called real-time evapotranspiration extension station installed in the potato field in a way not to interfere with the BLS beam path. A Campbell scientific enclosure was installed on the station tripod containing a data logger connected to the BLS SPU. A temperature and relative humidity sensor was installed at a height of 1.8 meters, a two way pyrradiometer sensor that measures the incoming and outgoing radiation was installed at an elevation of 2 meters above the canopy of the plants, a wind monitor sensor installed at an elevation of 2.5 meters, two temperature sensors were installed at 1.8 meters and 30 cm above the surface to measure the upper and lower temperature, and a soil heat flux plate (hukseflux) was installed at 8 cm below the ground to measure the soil heat flux that were all connected to the data logger, then, the data was send to the BLS SPU. The latter was programmed to store data at a 15minute averaging period using the SRun processing software provided by Scintec. The data was retrieved to a laptop after connecting it using an Ethernet cable. In this study, the latent heat and evapotranspiration were derived using the net radiation and the ground heat flux measured using the EC-SR tripod since more sensors were used in these techniques.

- **Boundary Layer Scintillometer Data Processing**

As a first step, the BLS measures the relative index of air using the following formula:

$$C_n^2 = 1.12\sigma_{\ln I}^2 D^{\frac{7}{3}} L^{-3} \quad (m^{-\frac{2}{3}})$$

Where $\sigma_{\ln I}^2$ is the variance of the natural logarithm of intensity fluctuations, and D and L are the aperture diameter and path length, respectively in meters.

Han et al. (2021) give the relation between the relative index of air and the temperature structure parameter from which the sensible heat flux can be calculated from MOST using the following equations:

$$C_T^2 = C_n^2 \left(\frac{T^2}{-0.78 * 10^{-6}} * 200\right)^2 \left(1 + \frac{0.003}{\beta}\right)^{-2}$$

$$\frac{C_T^2}{T_*^2}(Z_{LAS} - d)^{\frac{2}{3}} = f_T(\frac{Z_{LAS} - d}{L})$$

$$T * = -\frac{H}{\rho\, C_p u *}$$

$$u * = \frac{ku}{\ln\left[\frac{z_u - d}{Z_{0m}}\right] - \varphi_m\left[\frac{(z_u - d)}{L}\right] + \varphi_m(\frac{z_{0m}}{L})}$$

Where:

- $C_T$ is the temperature structure parameter in $(K^2/m^{-\frac{2}{3}})$
- T is the air temperature, $T_*$ is the temperature scale in kelvins
- P is the air pressure in pascals
- $\beta$ is the Bowen ratio (the ratio of Sensible Heat Flux to Latent Heat Flux).

- $Z_{LAS}$ is the observation height of the LAS, $d$ is the zero-plane displacement height, $L$ is the Obukhov length, $z_u$ is the observation height of wind speed, $Z_{0m}$ is the dynamic coarse roughness in meters
- $f_T$ is universal function related to atmospheric stability
- $H$ is the sensible heat flux in Watt per square meter
- $\rho$ is the air density in kilograms per cubic meter
- $C_p$ is the constant pressure of the specific heat in Joules per Kelvin * kg
- $u*$ is the friction wind speed in meters per second
- $\varphi_m$ is a modified function of momentum stability

The latent heat flux can be derived after obtaining the sensible heat flux using the energy balance equation:

$$LE = R_n - H - G$$

Where all in Watt per square meter, LE is the latent heat flux, $R_n$ is the net radiation, H is defined as above and G is the soil heat flux.

Figure 6 BLS 900 transmitter

Figure 7 BLS 900 receiver

### D. Statistical Analysis

In this paper, the Nash-Sutcliffe efficiency coefficient (NSE), percentage bias (PBIAS), coefficient of correlation (r) and determination ($R^2$), Root Mean Square Error (RMSE), Mean Bias Error (MBE), Mean and Standard deviation were used to study and compare the parameters measured and calculated by the EC, SR, and BLS.

$$r = \sum_{i=1}^{n} \frac{(a_i - a_{avg})(p_i - p_{avg})}{(a_i - a_{avg})^2 (p_i - p_{avg})^2}$$ (Pandey et al., 2020)

$$R^2 = 1 - \frac{\sum_{i=1}^{n} (a_i - p_i)^2}{\sum_{i=1}^{n} (a_i - a_{avg})^2}$$ (Chicco et al., 2021)

RMSE = $\sqrt{\frac{1}{n}(\sum_{i=1}^{n}(a_i - p_i)^2)}$ (Chicco et al., 2021)

NSE = 1 - $\frac{\sum_{i=1}^{n}(OBSi-SIMi)^2}{\sum_{i=1}^{n}(OBSi-\overline{OBS})^2}$ (Nash and Sutcliffe, 1970)

- $OBS_i$ is the observed value
- $SIM_i$ is the forecasted value
- OBS is the average observed values.

PBIAS = $\frac{\sum_{i=1}^{n}(pi-ai)}{\sum_{i=1}^{n}ai}$ (Tian et al., 2018)

MBE = $\frac{1}{n}\sum_{i=1}^{n}(p_i - a_i)$ (Alexandris et al., 2008)

- $a_i$ is the actual value
- $a_{avg}$ is the average actual values
- $p_{avg}$ is the average predicted values
- $p_i$ is the predicted value.

Mean = $\frac{Sum\ of\ Terms}{Number\ of\ Terms}$

Standard Deviation = $\sqrt{\frac{\sum(xi-u)^2}{N}}$

- N is the size of the population
- xi is each value from the population
- u is the population mean.

# CHAPTER IV

# RESULTS

## A. Descriptive Statistics

Table 1 shows the average and standard deviation of the sensible heat, latent heat and evapotranspiration measurements conducted at a half-hourly sampling frequency using each of the devices. EC sensible heat measurements surpassed those of SR by 44% while the percentage between EC and SR values and those of BLS were wider, with latter recording values almost twice as large. However, latent heat values for EC and SR showed good agreement with the latter only 3% higher, both devices also recorded the same ET value.

Moreover, the BLS had a 5.8 and 10 % higher latent heat and ET respectively than the EC recordings and resulted in an 18.1 and 23.1 % lower latent heat and ET values than SR. The standard deviation values showed a good agreement for sensible heat between the three devices. While SR had the greatest standard deviation for sensible heat, BLS had the highest SD value for latent heat and ET followed by SR and EC.

| **Half Hourly** | **Average** | | | **Standard Deviation** | | | **N** |
|---|---|---|---|---|---|---|---|
| | EC | SR | | EC | SR | | |
| **Sensible Heat (w/m$^2$)** | -7.1 | -13.1 | | 35.4 | 36.3 | | |
| **Latent Heat (w/m$^2$)** | 52.3 | 54.1 | | 79.8 | 116.5 | | 2547 |
| **ET (mm/half-hour)** | 0.04 | 0.04 | | 0.063 | 0.095 | | |
| | EC | SR | BLS | EC | SR | BLS | |
| **Sensible Heat (w/m$^2$)** | -5.8 | -13.7 | 7.8 | 47.5 | 36.3 | 35.9 | |
| **Latent Heat (w/m$^2$)** | 123.5 | 160 | 131 | 95.2 | 116.5 | 133 | 867 |
| **ET (mm/half-hour)** | 0.09 | 0.13 | 0.1 | 0.076 | 0.11 | 0.11 | |

Table 1 Half-hourly sensible heat, latent heat and evapotranspiration descriptive statistics

Table 2 offers the same descriptive statistics for the hourly sampling. The results are almost identical to the half hourly sampling with the exception of slightly increased ET values.

| **Hourly** | **Average** | | | **Standard Deviation** | | | **N** |
|---|---|---|---|---|---|---|---|
| | EC | SR | | EC | SR | | |
| **Sensible Heat (w/m$^2$)** | -7.1 | -13.1 | | 34.5 | 34.8 | | |
| **Latent Heat (w/m$^2$)** | 52.3 | 54.1 | | 79.1 | 113.6 | | 1276 |
| **ET (mm/hour)** | 0.09 | 0.09 | | 0.13 | 0.18 | | |
| | EC | SR | BLS | EC | SR | BLS | |
| **Sensible Heat (w/m$^2$)** | -6.5 | -14.1 | 7.2 | 45.9 | 44.4 | 34.4 | |
| **Latent Heat (w/m$^2$)** | 119.9 | 154.5 | 126.3 | 94.1 | 127.6 | 129.1 | 452 |
| **ET (mm/hour)** | 0.19 | 0.25 | 0.2 | 0.15 | 0.2 | 0.2 | |

Table 2 Hourly sensible heat, latent heat and evapotranspiration descriptive statistics

Table 3 offers descriptive statistics for EC and SR measurements conducted daily. The values for latent heat and ET are in good agreement, as in previous cases, with a 3% higher value for latent heat shown by EC and less than a 1% higher value by EC for ET. while the difference between sensible heat values narrowed to a 41% larger recording by EC. The standard deviation values, however, record closer values for the two devices than in more granular samplings.

| **Daily** | **Average** | | **Standard Deviation** | | **N** |
|---|---|---|---|---|---|
| | EC | SR | EC | SR | |
| **Sensible Heat (w/m$^2$)** | -7.2 | -12.2 | 13.9 | 13.7 | |
| **Latent Heat (w/m$^2$)** | 52 | 50.2 | 24 | 26.9 | 58 |
| **ET (mm/Day)** | 2.0 | 1.9 | 1.0 | 0.9 | |

Table 3 Daily sensible heat, latent heat and evapotranspiration descriptive statistics

The statistics for weekly sampling shown in table 4 are similar to those in table 3 except the difference between the EC and SR sensible heat average narrowed further to a 38.5% higher value by the latter, while a slightly larger difference was found for latent heat averages with SR values being 4% lower than EC. The comparison of standard deviations was again consistent with previous results.

| **Weekly** | **Average** | | **Standard Deviation** | | **N** |
|---|---|---|---|---|---|
| | EC | SR | EC | SR | |
| **Sensible Heat (w/m$^2$)** | -6.7 | -10.9 | 8.8 | 9.9 | |
| **Latent Heat (w/m$^2$)** | 50.8 | 48.4 | 21.2 | 23.8 | 9 |
| **ET (mm/Week)** | 13.6 | 12.9 | 5.7 | 6.3 | |

Table 4 Weekly sensible heat, latent heat and evapotranspiration descriptive statistic

### B. Time of day variations in latent heat, evapotranspiration & sensible heat

Figure 8 shows radar plots comparing the average values for LE and ET as they vary throughout the day. In October, all three devices record the maximum LE at 1pm, nearing 400W/$m^2$ for SR, followed by BLS at close to 350 W/$m^2$ and EC slightly below 300 W/$m^2$. In November, LE values reach their maximum for SR and BLS at 1pm as well at almost halved values nearing 250 W/$m^2$ and slightly over 200 W/$m^2$, respectively, while EC reaches its maximum later also at a lower value than the previous month at slightly over 150 W/$m^2$. In December, LE drops further down reaching an earlier maximum of 200 W/$m^2$ for SR at 12pm and a late, also decreased maximum of 100 W/$m^2$ for EC. The values for ET show similar temporal trends for the three months, reaching maxima at the same time as for LE values. While remaining similarly elevated across October and November, the values drop sharply in December.

Figure 9 compares the devices' hourly recordings of H. BLS records the greatest sensible heat in October at 10am reaching 24.2 W/$m^2$ then at 11am in November at 48.4 W/$m^2$. SR reaches a maximum of H at 9am at 9.5 W/$m^2$ then in November at 2pm of 7.6 W/$m^2$ and peaking in December at 12pm reaching 110.62 W/$m^2$. EC reaches peak H in October at 11am recording 19.27 W/$m^2$ then shows similar values to SR in November with a slightly higher peak of 10.64 W/$m^2$ at 1pm and then jumping to a maximum of 215.6 W/$m^2$ at 1pm in December.

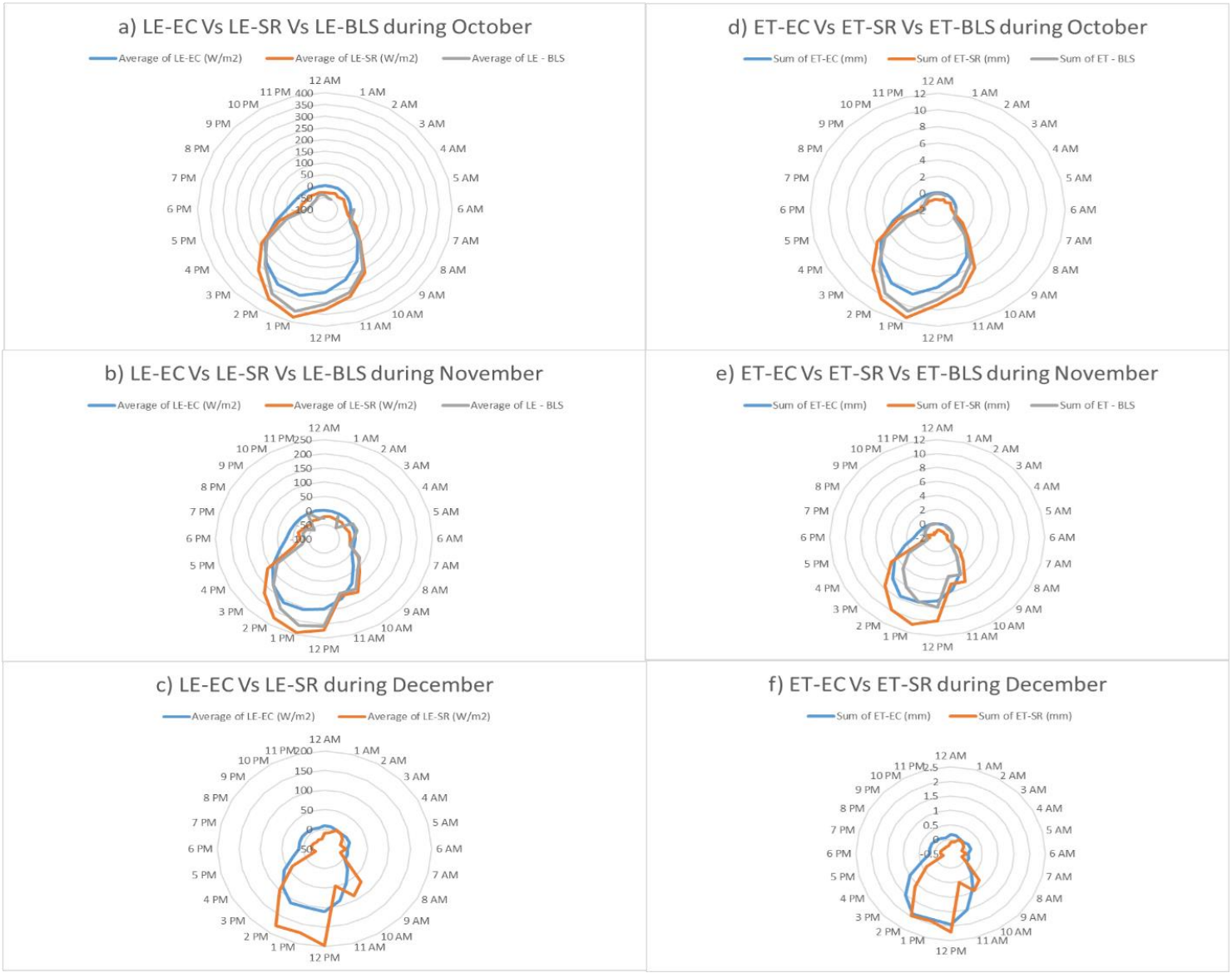


Figure 8 Average hourly value EC, BLS and SR intercomparison for latent heat flux (LE) and evapotranspiration (ET)

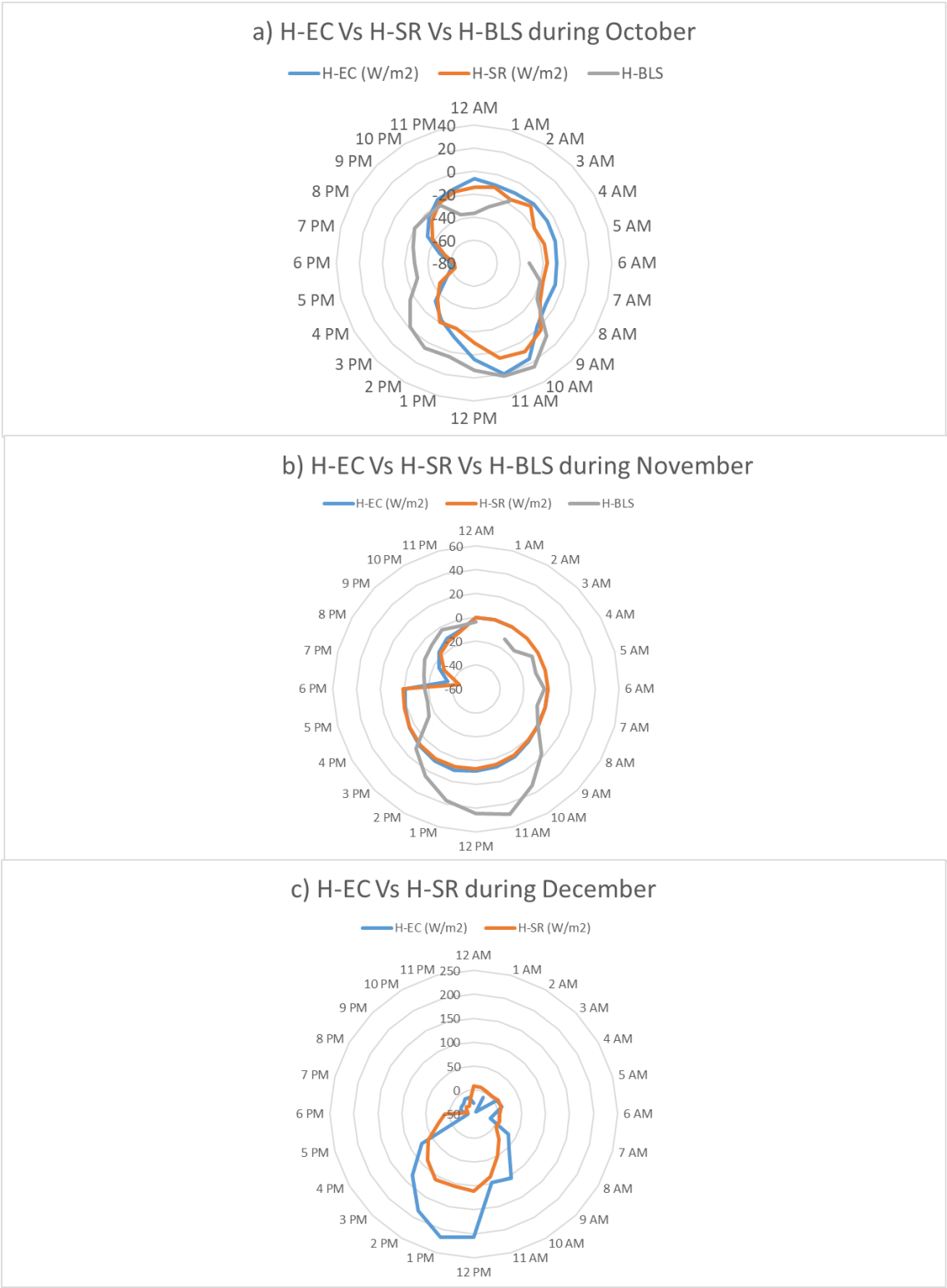


Fi

Figure 9 Average hourly value EC, BLS and SR intercomparison for sensible heat flux (H)

### C. Impact of wind speed and direction on sensible heat

Figure 10 shows the influence of wind speed and sonic wind direction, which has an angle of 0 to the North and increases clockwise, on sensible heat measured by Scintillometry compared to the values obtained using Eddy Covariance. We can see that when the wind direction is perpendicular to the beam path of the BLS (between the angles of 0 to 90 or 180 to 270 degrees), the percent mean difference is lower than when the wind is blowing in other directions. We can also notice that the percentage mean difference is the lowest when the wind speed is high due to the uniformity on air parcels size (1 to 5 m/s). The sensible heat values for both devices remained cohesive in most other scenarios.

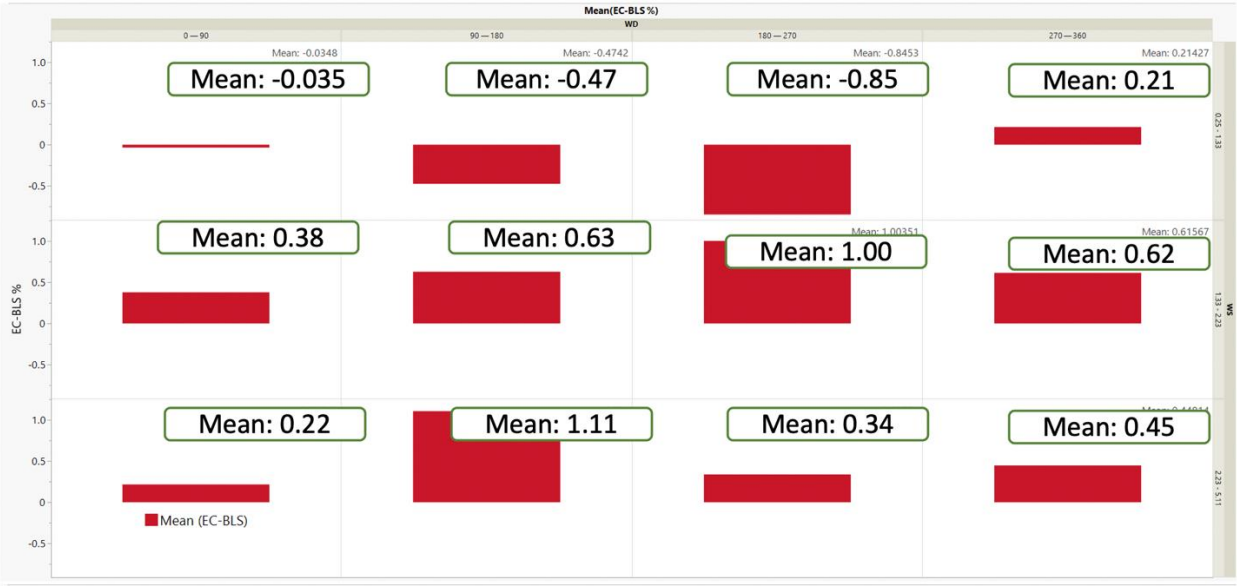


Figure 10 Percent Difference of mean H (EC) compared to mean H (BLS) ($W/m^2$) with respect to Wind Speed (m/s) and Sonic Wind Direction (º)

Figure 11 also examines the difference in sensible heat measurement caused by wind speed and direction, comparing the magnitude of the means using EC and SR.

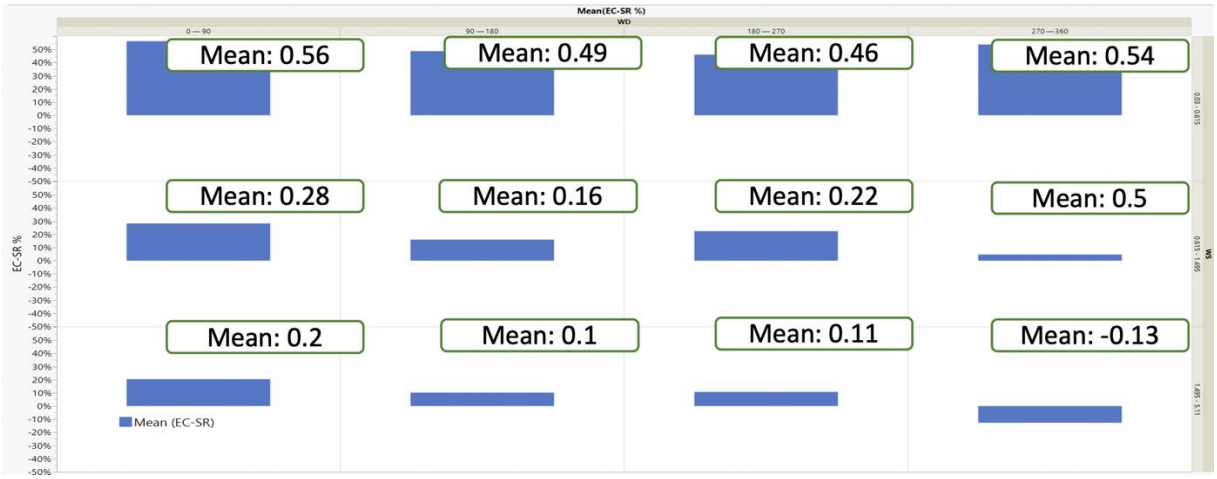


Figure 11 Difference of mean H (EC) (W/m$^2$) and mean H (SR) (W/m$^2$) with respect to Wind Speed (m/s) and Sonic Wind Direction (º)

### D. Time series plots

No daily and weekly H-BLS were plotted since the BLS-900 skipped 60% of its data.

### 1. Half hourly measurements

Figure 12 shows sensible heat, latent heat and evapotranspiration using half hourly measurements from EC (orange), BLS (blue) and SR (gray). The values are in good

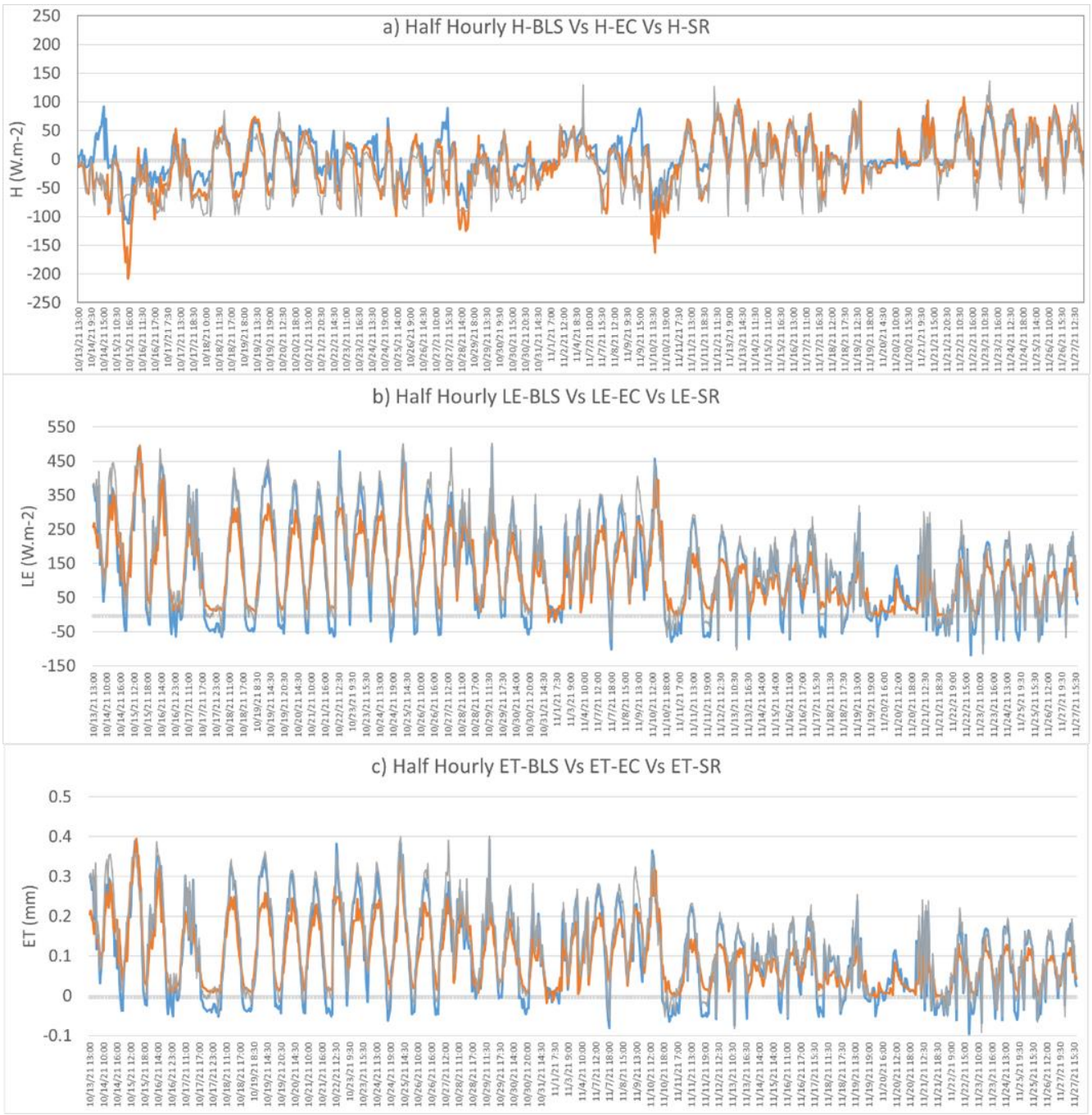


Figure 12 Intercomparison between BLS and SR values for sensible heat, latent heat and evapotranspiration using half hourly measurements

agreement for the majority of measurements, except for peak hours during which BLS is significantly higher. EC measurements occasionally drop below other techniques, also during peak hours. H measured by SR tends to fall below EC and BLS measurements during nadirs. BLS measured H was 33% higher than from EC and 37% higher than using SR, while SR measured H was 58% lower than EC.

BLS measurements for LE and ET have consistently greater magnitudes than other techniques, which agree for a majority of measurements. Overall, BLS values for both LE and ET were only 6% greater than using EC and 13% lower than SR derived LE and ET, while EC values were 18% percent lower than those found using SR.

### 2. Hourly Aggregation

Figure 13 shows sensible heat, latent heat and evapotranspiration using hourly measurements from EC (orange), BLS (blue) and SR (gray). H using EC measurements was on average 10% lower than through BLS measurements and 51% greater than SR measurements. Meanwhile, H from SR measurements was 45% smaller than BLS. The results showed closer agreement for LE and ET, with BLS values only 5% greater than those from EC and 13% lower than those found using SR while EC values were 18% lower than those found using SR.


Figure 13 Intercomparison between EC, BLS and SR values for sensible heat, latent heat and evapotranspiration using hourly measurements

### 3. Daily Aggregation

Figure 14 shows the different sensible and latent heat values found using EC and SR through daily measurements. H values using EC were on average 41% greater than those found using SR, while LE and ET values showed good agreement with EC values only 3% greater than SR values.

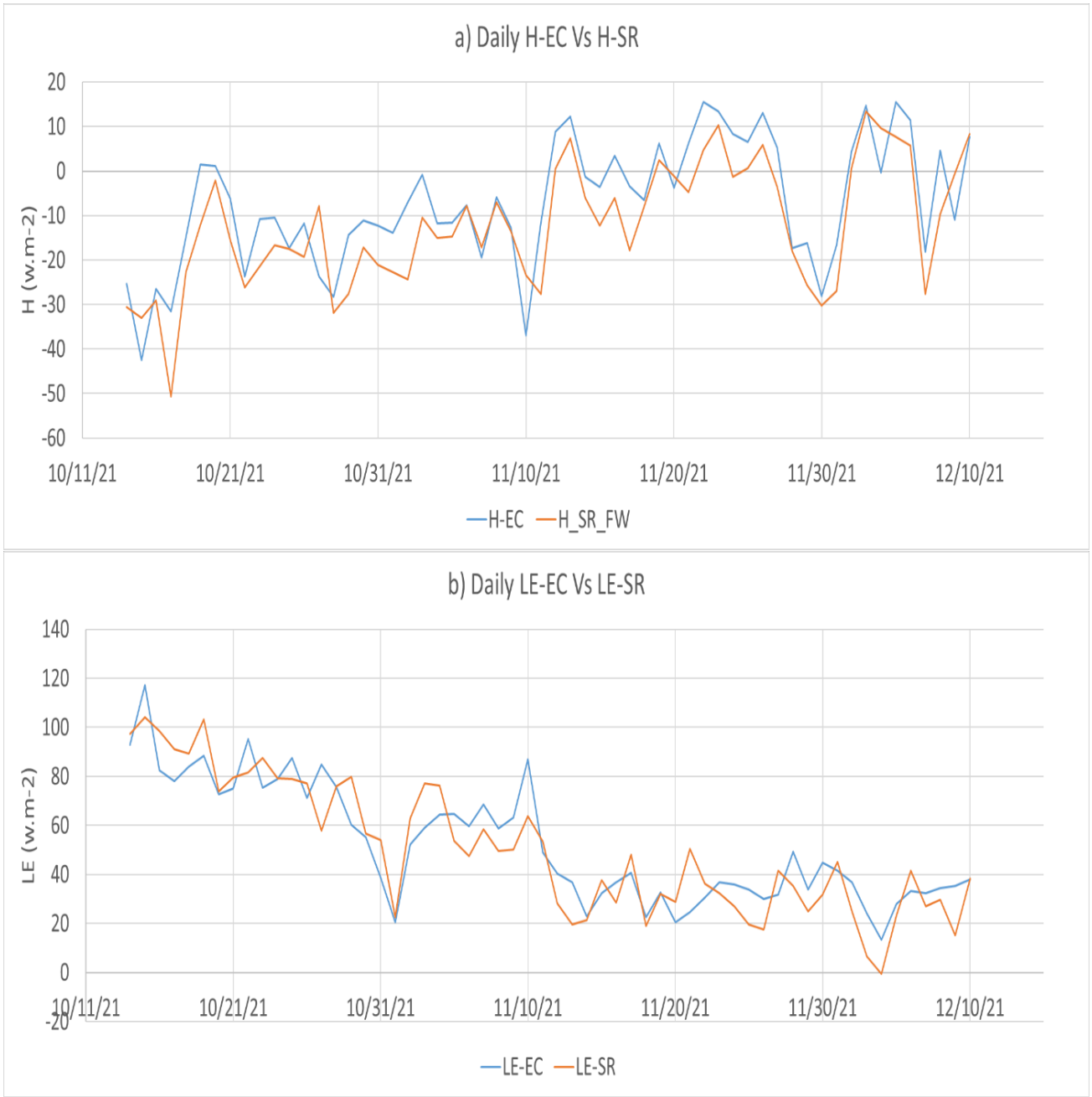


Figure 14 Intercomparison between EC and SR values for sensible and latent heat using daily measurements

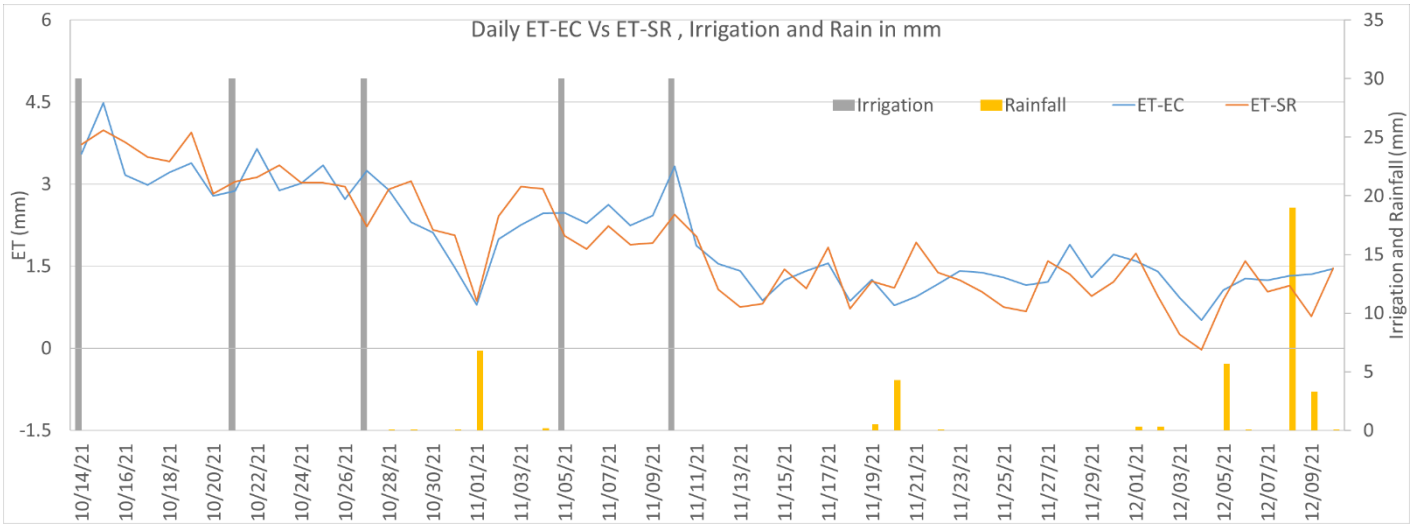


Figure 15 Comparison of evapotranspiration values obtained using daily sampling of EC and SR along with irrigation and rain estimates

Figure 15 shows the different ET values obtained using EC and SR along with dates of irrigation and rain events. The difference between values does not exceed 3% as mentioned above, however additionally visible is the lack of disturbance caused by rainfall and irrigation on the agreement between values. The sum of ET-EC during the measurement period was 115.4 mm while the sum of ET-SR was 111.5 mm. The total irrigation depth during the same period was 191 mm which is 41.7% higher than ET-SR and 39.8% from ET-EC. Taking into consideration that not all the water applied will be used by the plants due to soil moisture storage, infiltration, and the irrigation drift, the total irrigation depth was relatively high. The latter can be reduced to assess its impact on productivity.

## 4. Weekly Aggregation

Figure 16 compares H, LE and ET values found by EC and SR using weekly measurements. The results were similar to those found using daily values, as EC values for H were 42% greater than those found using SR while LE and ET values were only 4% greater.

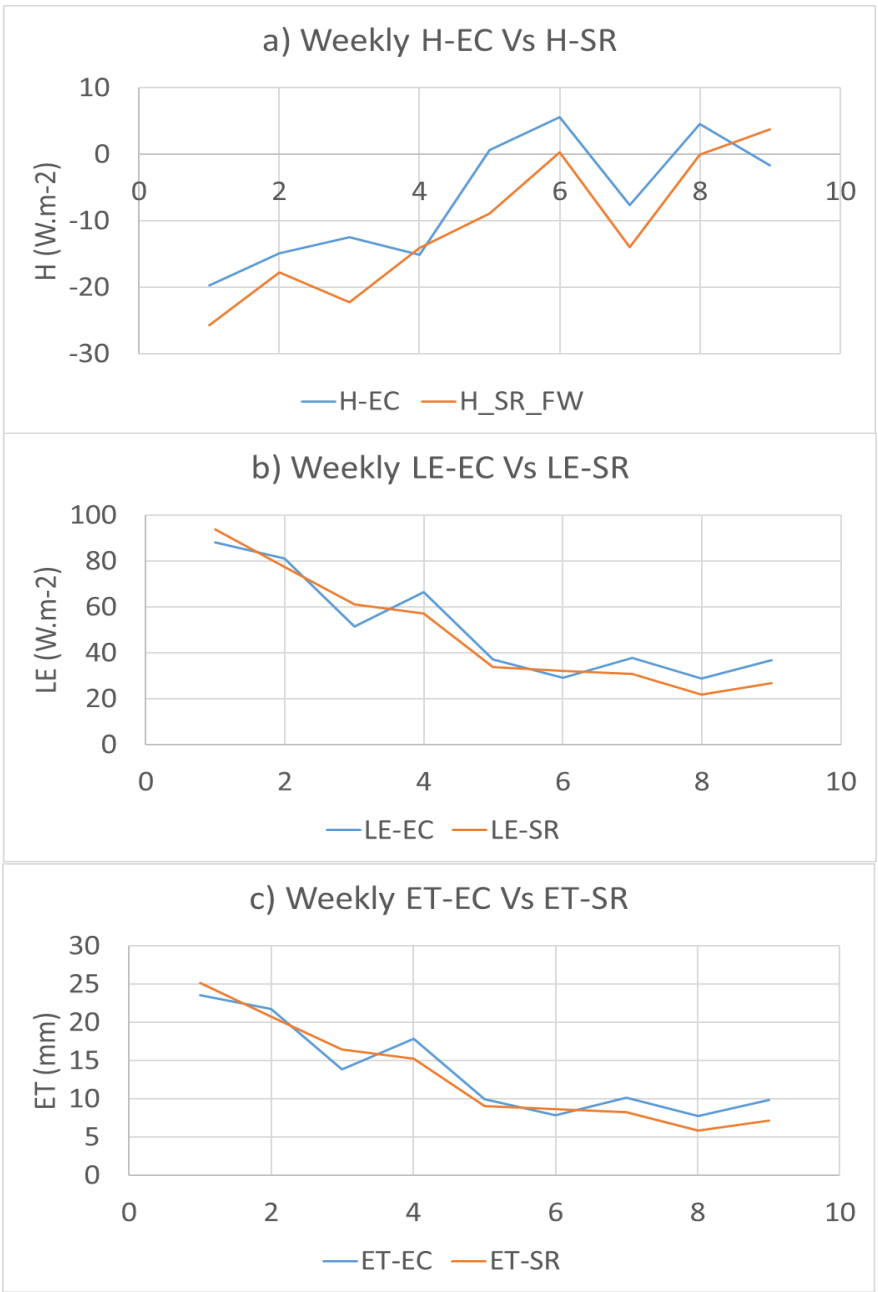


Figure 16 Intercomparison between EC and SR values for sensible heat, latent heat and evapotranspiration using weekly measurements

### E. Statistical analysis and scatter plots

Figure 17 displays the statistical analysis conducted on the different measurements. Figures 18-21 represent scatter plot representations of the comparison between techniques at different sampling rates. The best correlation was found between values for H and LE through SR and EC using weekly measurements.

| Values | R | | R2 | | RMSE (W.m-2) | | NSE | | Pbias (%) | | MBE (W.m-2) | |
|---|---|---|---|---|---|---|---|---|---|---|---|---|
| | H | LE | H | LE | H | LE | H | LE | H | LE | H | LE |
| Half-Hourly SR vs EC | 0.77 | 0.92 | 0.59 | 0.84 | 23.51 | 54.71 | 0.57 | 0.57 | -6.79 | -0.04 | -5.39 | -1.23 |
| Hourly SR vs EC | 0.85 | 0.93 | 0.72 | 0.87 | 20.11 | 48.61 | 0.67 | 0.65 | -0.05 | 0.38 | -5.4 | -1.24 |
| Daily SR vs EC | 0.87 | 0.89 | 0.75 | 0.8 | 8.68 | 11.76 | 0.6 | 0.76 | -0.0005 | 0.001 | -5.05 | -1.78 |
| Weekly SR vs EC | 0.88 | 0.96 | 0.78 | 0.93 | 6.23 | 7.01 | 0.51 | 0.89 | 0.001 | 0.004 | -4.22 | -2.42 |
| Half-Hourly BLS vs EC | 0.82 | 0.9 | 0.68 | 0.81 | 30.17 | 63.9 | 0.6 | 0.55 | -0.22 | 0.044 | 13.62 | 7.46 |
| Hourly BLS vs EC | 0.85 | 0.92 | 0.73 | 0.85 | 27.89 | 56.12 | 0.63 | 0.64 | 1.42 | 0.23 | 13.79 | 6.38 |

Figure 17 Statistical parameters comparing H and LE values from each technique at various sampling rates

Correlation did not fall below 0.89 for LE measurements using the different techniques at all frequencies while the lowest correlation was recorded for H measurements from SR and EC using half-hourly data. The coefficient of determination showed similarly good values for LE with the highest $R^2$ at 0.93 relating weekly measurement derived LE for SR and EC and the lowest at 0.8 comparing LE found by EC and SR using daily measurements. $R^2$ was lower for H, with the lowest value at 0.59 between half hourly data derived values of SR and EC and the highest at 0.78 for weekly data from SR and EC. The highest RMSE was found for the comparison between half-hourly sampled BLS and EC measurements for LE values at 63.9 $W/m^2$ while the lowest RMSE for LE values were

for the weekly sampled SR and EC values at 7.01 W/m$^2$. The same technique comparisons and sampling frequencies resulted in the highest and lowest RMSE values for H measurements at respectively 30.17 W/m$^2$ and 6.23 W/m$^2$. MBE values varied for H measurements between -5.04 W/m$^2$ for hourly measurement derived values using SR and EC and 13.79 W/m$^2$ for hourly sampled BLS and EC. Meanwhile LE measurement MBE values differed between -2.42 W/m$^2$ for weekly sampled SR and EC measurements and 7.46 W/m$^2$ for half-hourly sampled BLS and EC measurements. PBIAS values were close to 0 for half-hourly sampled SR compared to EC measurements of LE and BLS compared to EC and daily sampled SR and for which PBIAS for LE values were also close to 0. The greatest PBIAS for H values was recorded for half hourly SR and EC sampling and for LE values the greatest PBIAS came from comparing half-hourly sampled BLS and EC estimates. Weekly sampled SR and EC values had the greatest NSE values for LE at 0.89, while the remainder of values did not surpass 0.65 with the exception of daily SR vs EC at 0.76. For H, none of the values surpassed 0.67, the maximum recorded by the comparison of hourly sampled SR and EC values.

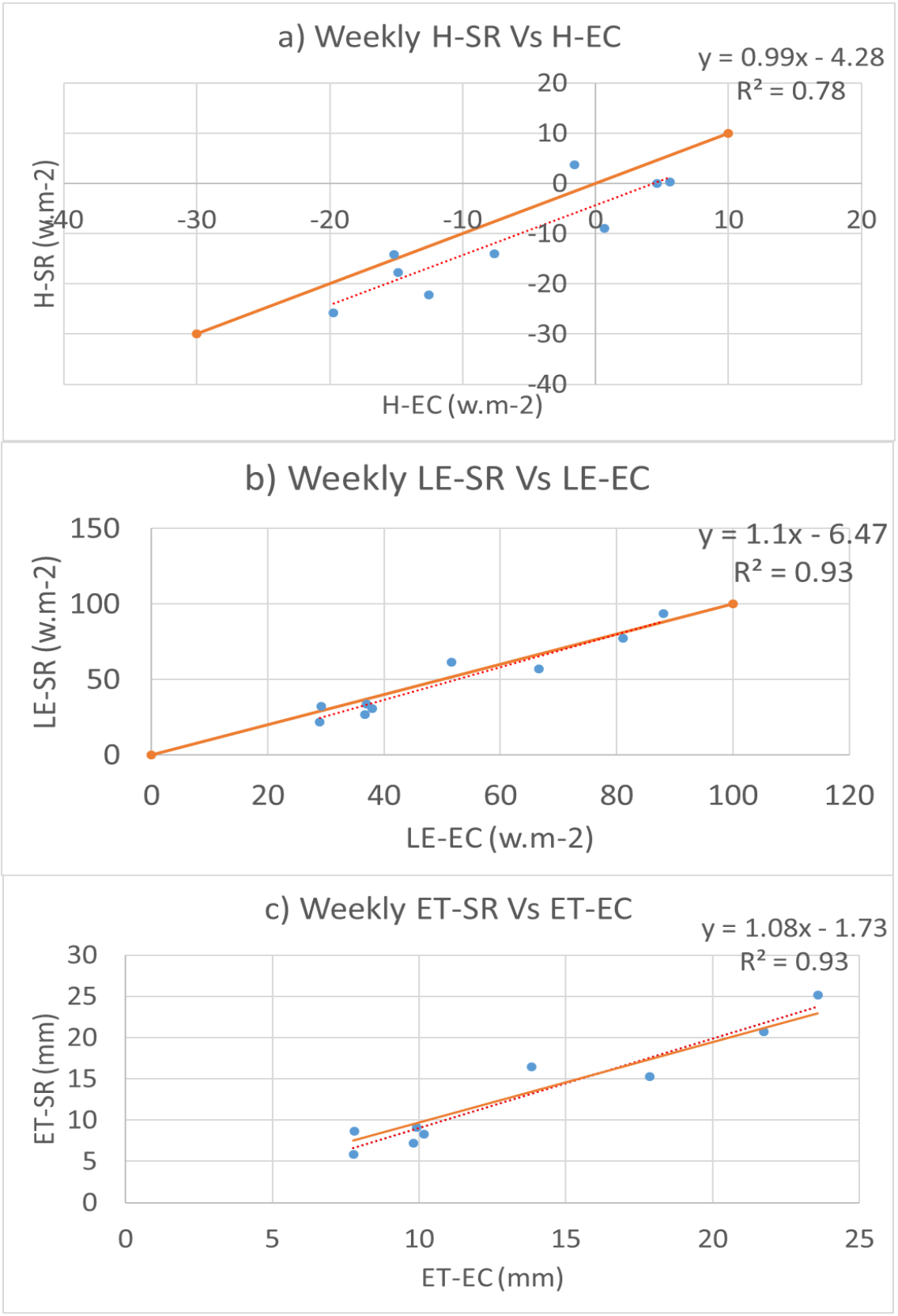


Figure 18 Scatter plot comparing H, LE and ET values using weekly measurements for each technique

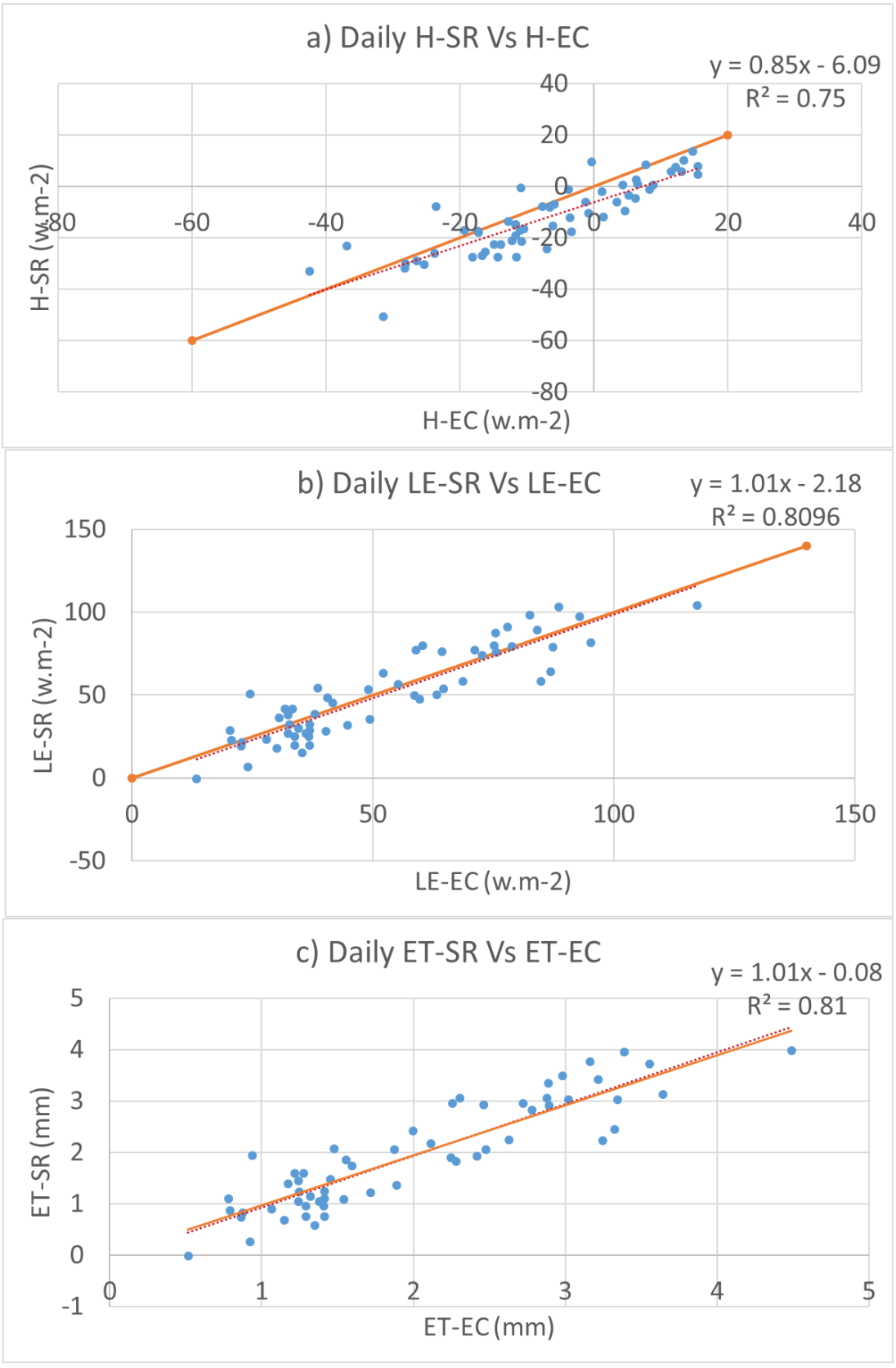


Figure 19 Scatter plot comparing H, LE and ET values for daily measurements using each technique

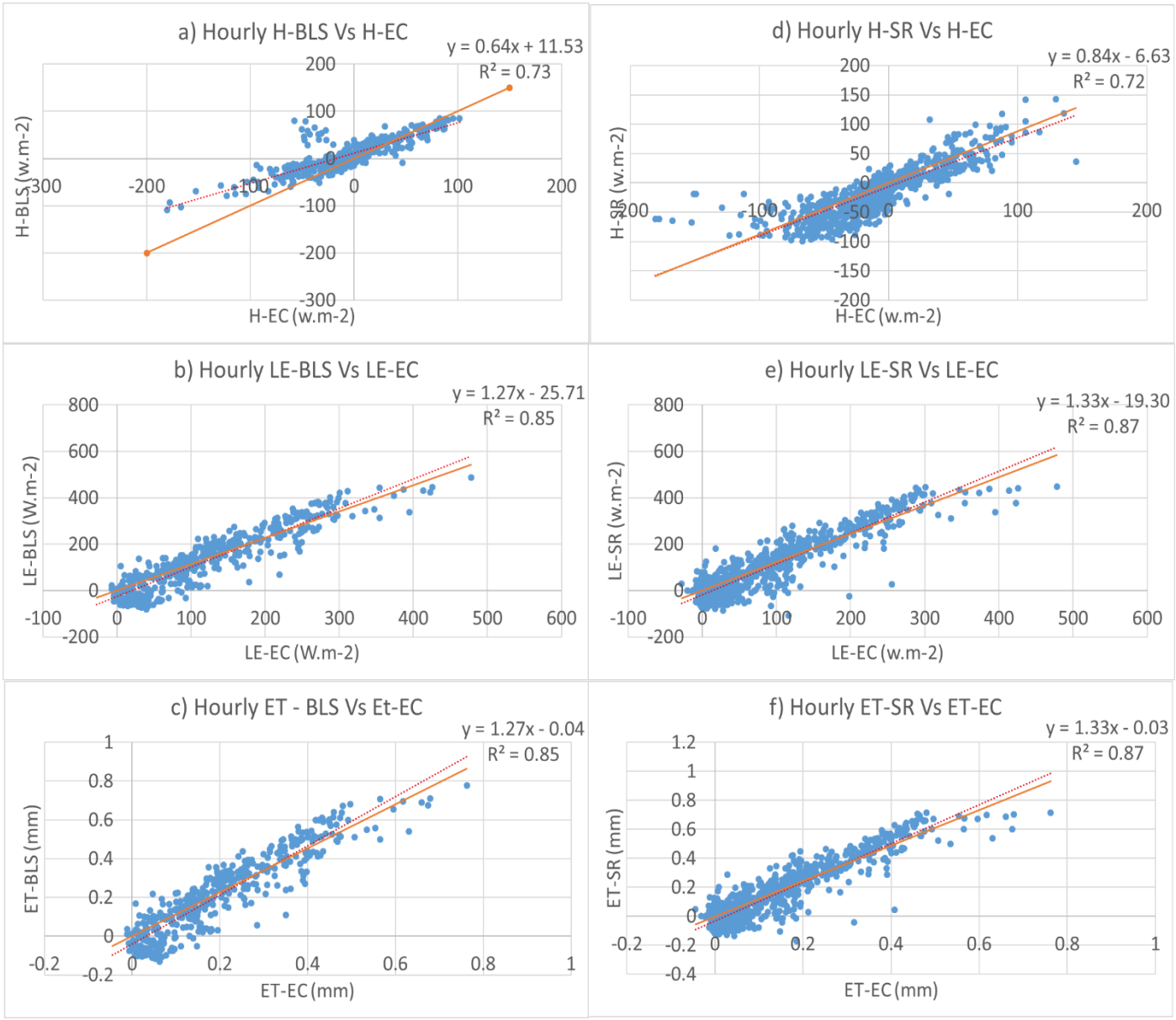


Figure 20 Scatter plots comparing H, LE and ET values for each technique using hourly measurements

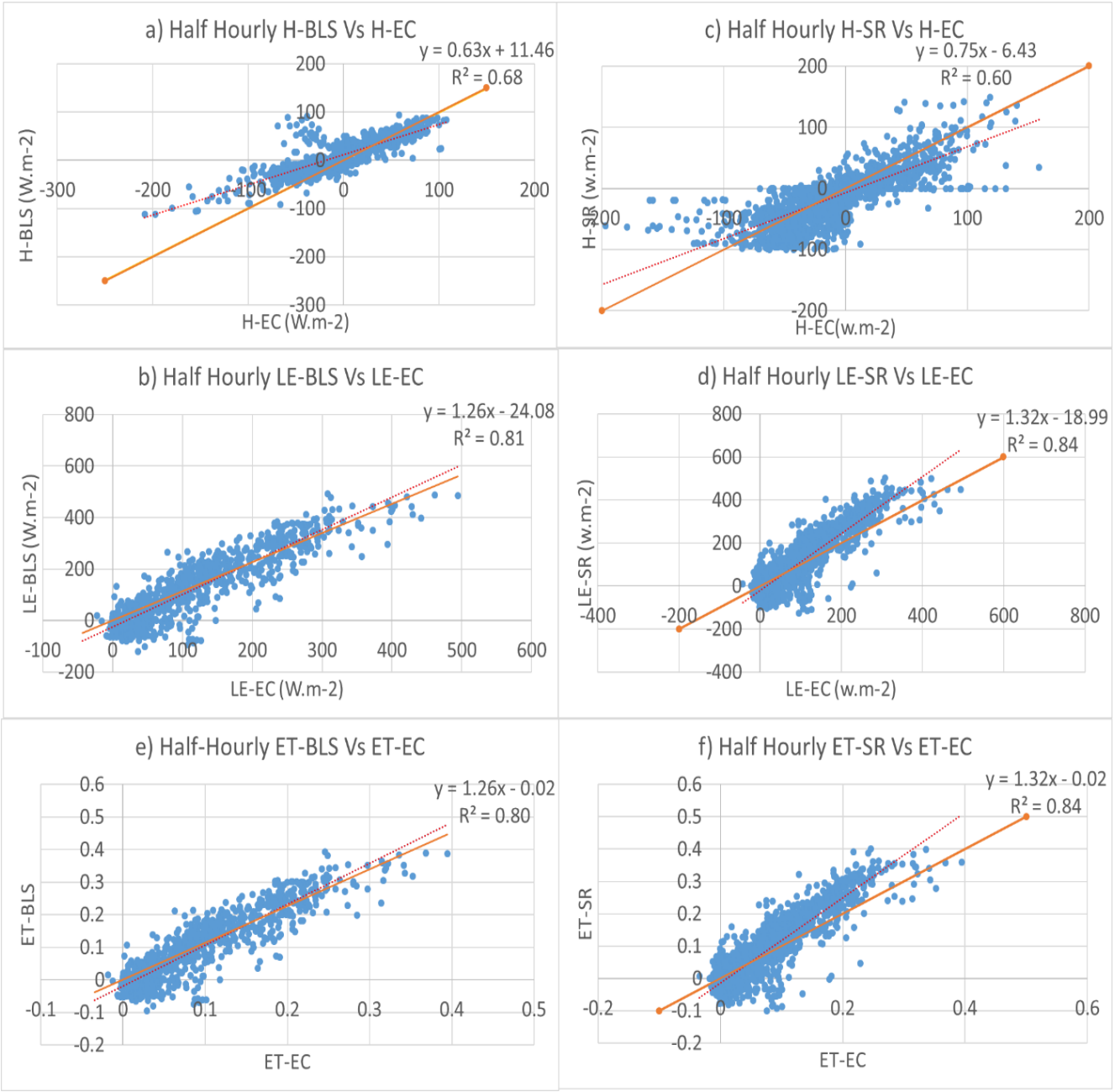


Figure 21 Scatter plots comparing H, LE and ET values for each technique using half-hourly measurements

### F. Statistical Analysis and Scatter Plot Excluding Time Factor

Table 5 represents the correlation coefficient which is the strength of the relationship among the sensible heat collected from the three systems after removing the time factor,

along with the number of reading collected, the root mean square error, and the mean bias error. The sensible heat results show satisfying correlation for SR vs EC with a maximum R of 0.82 between 12 and 1 pm while the RMSE is equal to 26.8 w/m$^2$ and the MBE is -10.03 w/m$^2$. On the other hand, a minimum value of R was between the hours of 4 and 5 pm and equal to 0.5 with RMSE 35.34 w/m$^2$ and the MBE -8.04 w/m$^2$. The number of readings were consistent during the whole measurement period. As for BLS vs EC, the maximum coefficient of correlation was 0.89 between the hours of 6 and 7 am a value of RMSE equal to 12.98 w/m$^2$ and the MBE is 10.56 w/m$^2$, and the minimum was 0.1 between 2 and 3 am while RMSE is equal to 21.59 w/m$^2$ and the MBE is 15.39 w/m$^2$. It is important to note that the number of readings in BLS vs EC is much lower than SR vs EC since the BLS skipped 60% of the readings.

| Hours | BLS vs EC | | | | SR vs EC | | | |
|---|---|---|---|---|---|---|---|---|
| | N | R | RMSE (w.m-2) | MBE (w.m-2) | N | R | RMSE (w.m-2) | MBE (w.m-2) |
| 0-1 | 5 | 0.89 | 27.98 | 23.92 | 208 | 0.72 | 16.06 | -3.80 |
| 2-3 | 11 | 0.10 | 21.59 | 15.39 | 212 | 0.74 | 15.69 | -4.39 |
| 4-5 | 8 | 0.57 | 10.90 | 6.33 | 212 | 0.48 | 20.11 | -4.38 |
| 6-7 | 15 | 0.89 | 12.98 | 10.56 | 212 | 0.67 | 16.74 | -5.15 |
| 8-9 | 80 | 0.73 | 16.85 | 11.26 | 212 | 0.56 | 14.12 | 0.85 |
| 10-11 | 166 | 0.77 | 18.50 | 4.03 | 212 | 0.71 | 25.67 | -4.11 |
| 12-13 | 165 | 0.83 | 28.43 | 5.59 | 214 | 0.82 | 26.80 | -10.03 |
| 14-15 | 159 | 0.69 | 41.60 | 16.89 | 216 | 0.80 | 33.22 | -10.66 |
| 16-17 | 138 | 0.64 | 35.23 | 21.54 | 213 | 0.50 | 35.34 | -8.04 |
| 18-19 | 75 | 0.61 | 31.94 | 26.91 | 212 | 0.48 | 28.44 | -7.87 |
| 20-21 | 30 | 0.81 | 33.51 | 30.01 | 212 | 0.69 | 20.60 | -3.63 |
| 22-23 | 15 | 0.83 | 21.64 | 16.39 | 212 | 0.77 | 16.16 | -3.27 |

Table 5 Statistical analysis after removing time factor

## G. Energy balance closure

Figures 22 and 23 offer statistical analyses to determine the energy balance closure results, comparing the sum of latent and sensible heat fluxes (LE+H) and the difference between the net radiation and soil heat flux ($R_n$-G). The different sampling rates showed consistently good results for R which was at 0.96 for hourly sampling and 0.94 for other values and $R^2$ which stood between 0.82 for daily sampling and 0.93 for hourly sampling. The RMSE varied between 48.76 and 43.51 for half-hourly and hourly sampling, respectively, and 11.20 and 7.91 for daily and weekly sampling, respectively. PBIAS was close to 0 for all sampling rates except for half-hourly in which the measure was at -2.14%. MBE values were close for all rates, slightly varying between 6.82 for half-hourly sampling and 5.71 for weekly sampling. NSE values ranged between 0.84 for half-hourly sampling and 0.77 for weekly obtained values.

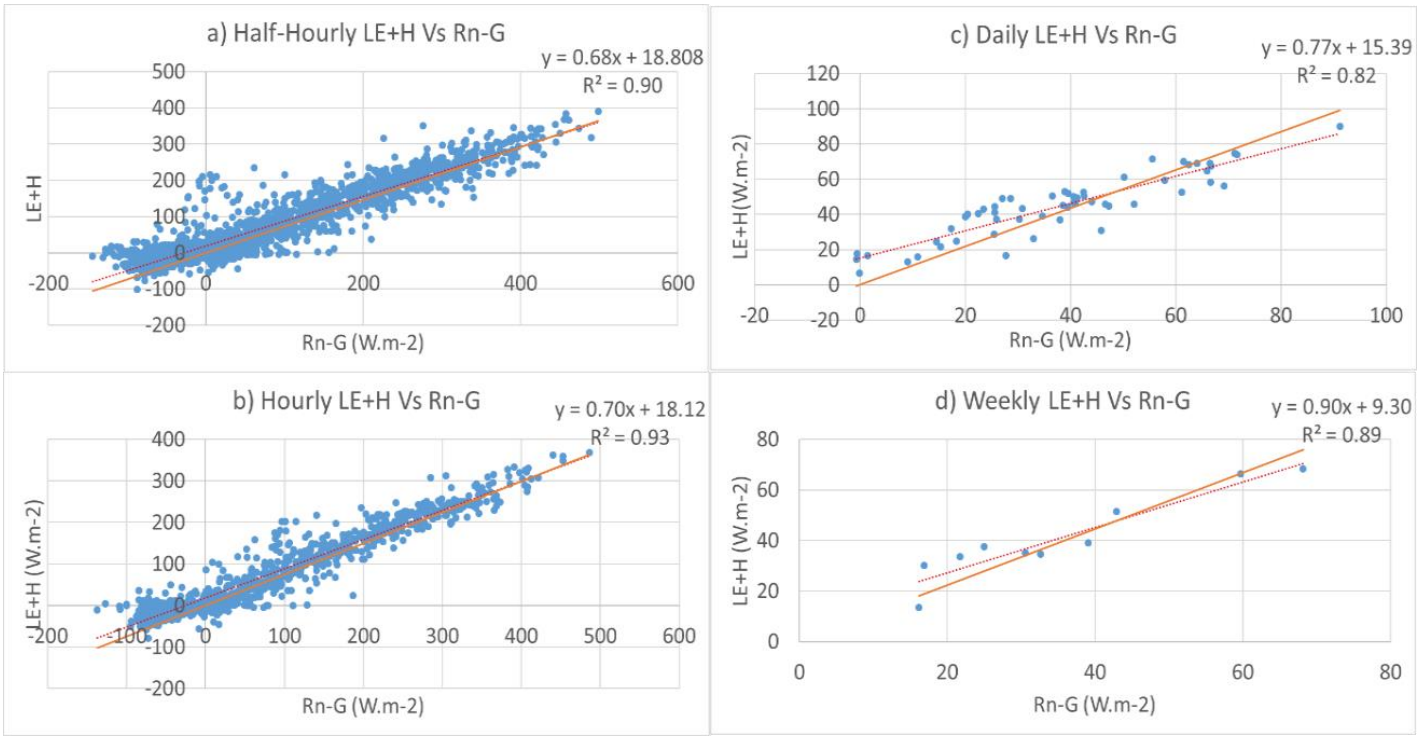


Figure 22 Energy balance closure scatter plots for different sampling rates

| Values | R | R2 | RMSE (W.m-2) | NSE | Pbias (%) | MBE (W.m-2) |
|---|---|---|---|---|---|---|
| **Half-Hourly LE+H vs Rn-G** | 0.94 | 0.89 | 48.76 | 0.84 | -2.14 | 6.65 |
| Hourly LE+H vs Rn-G | 0.96 | 0.93 | 43.51 | 0.87 | -0.55 | 6.67 |
| Daily LE+H vs Rn-G | 0.94 | 0.82 | 11.2 | 0.71 | 0.0002 | 6.82 |
| Weekly LE+H vs Rn-G | 0.94 | 0.9 | 7.91 | 0.77 | 0.003 | 5.71 |

Figure 23 Statistical description of energy balance closure comparison for each sampling rate

# CHAPTER V

# DISCUSSION

## A. Sensible Heat

H measurements from BLS were found to be especially sensitive to wind compared to EC, which were also on average greater, in agreement with previous works (Li et al., 2017; Zhao et al., 2016). Similarly, H values from SR measurements were also consistently lower than both other devices. The readings could be affected by the fetch as shown in the chapter IV (section C). The wind impact is consistent with Haymann et al. (2018) who concluded that H (EC) might increase as it requires a higher fetch. The difference in sensible heat flux estimation can also be linked to surface energy balance closure errors (Vendrame et al., 2020) and, for SR, possible errors in sensor calibration or error in the calibration factor for H (Gray et al., 2021).

The determination coefficient for sensible heat from half-hourly measures from each of BLS and EC found in the current study falls under that found by Ezzahar et al. (2007) for daily averaged values, furthermore, the hourly coefficient matches their research. Ezzahar et al. (2007) compared daily averaged measurements from Scintillometry and Eddy Covariance over a 275 hectares' olive yard in a semi-arid region, finding a $R^2$ of 0.72 for H. The $R^2$ value found comparing between H from half-hourly measurements for BLS and EC, however, matched the value found by Liu et al. (2010) at the same sampling rate between 0.65 and 0.67. The results however fall significantly below the comparisons made by Vendrame et al. (2020) consistently finding $R^2$ values above 0.95 when comparing Scintillometers and EC, a result also found by Zhao et al. (2016).

Meanwhile, the low $R^2$ values for the comparison between Scintillometry and Surface Renewal sensible heat found in the current study are below the values determined around 0.8 by Wang et al. (2021) and identified in Hu et al.'s (2018) review in which only three studies had a value below 0.8. While still pointing towards a good correlation, the reduced values can be linked to the humidity conditions (Hu et al., 2018).

### B. Latent Heat

The LE values found using EC and BLS were in good agreement, with the latter only slightly smaller than the former. The consistent agreement of results across the entire experiment duration comes despite the monthly variation of peak times and the sensitivity of measurements of heat flux to peak value found in the current study. The difference may be due to the underestimation of LE by the EC system which has been previously observed (Pozníková et al., 2018), errors in sensor calibrations and their height above the canopy and discrepancies in the net radiation and ground heat flux measurement (Hu et al., 2018), or by the energy balance closure errors (Vendrame et al, 2020).

Similarly, SR derived LE values mostly agreed with the other techniques examined.

The comparison between EC and SR for LE $R^2$ values outperformed some of the literature values identified, slightly above Ezzahar's (2017) determined $R^2$ of 0.76.

The high $R^2$ values found for LE during a comparison of EC and SR values is consistent with the literature (Wang et al., 2021 ; Hu et al., 2018 ; Castellvì et al., 2006).

The SR and BLS derive LE using the surface balance equation, therefore, any bias in the measurement of H, G, and $R_n$ can affect LE-BLS measurements.

### C. Evapotranspiration

All three techniques showed good agreement on evapotranspiration values with only slight differences in average results at all sampling frequencies. Similarly, consistently high $R^2$ values were found in comparisons between ET values for different techniques. Poznikovà et al. (2018) found that Scintillometry and SR showed consistently good results in agreement with each other compared to underestimates from EC.

The difference may be caused by the bias in sensible heat flux estimation as it is affected by the wind speed, wind direction, and the energy balance closure error.

### D. Energy balance closure

The energy balance closure $R^2$ values are in agreement with the literature, including Ezzahar's (2007) finding of 0.86 and Liu et al. (2010) finding values between 0.86 and 0.93. The difference may be caused by unaccounted energy losses, inadequate accounting of other storage terms (Allen et al., 2011), or errors or biases in the measurements of $R_n$, G, and the turbulent fluxes (Bambach et al., 2022), especially that soil moisture sensors, thermocouples, and soil heat flux plates were installed in the middle of the field which may not represent the whole area of study. Therefore, more sensors may be needed to result in more accurate heat flux measurements which will need more sophisticated methods and cost.

# CHAPTER VI

# CONCLUSION AND RECOMMENDATIONS

This study compared Eddy Covariance, Surface Renewal and Boundary Layer Scintillometry as different options to determine heat fluxes and evapotranspiration in agricultural land. This experiment was conducted over a potato field in the Bekaa Valley between in the fall of 2021. All three techniques showed good agreement and high correlation for latent heat and evapotranspiration. Sensible heat measurements remained more variable among some techniques due to the sensitivity to wind along with the individual features of each measurement tool. Our findings were overall consistent with previous work, with the added novelty of offering a unified comparison between the three techniques.

In conclusion, with accurate measurements of ground heat flux and net radiation, the BLS can be a reliable system for measuring sensible heat fluxes in semi-arid region, but omits a high percentage of data (60%) due to power supply, alignment, and climate conditions. While for EC, the energy balance closure and the fetch requirements of the system must be studied to ensure accurate measurement. Although, the SR is a new reliable system, more durable fine wires should be manufactured to fit with field conditions. Moreover, the calibration of the sensors and the data post processing must be improved.

A key finding is to note the different techniques all proved reliable, paving the way for greater flexibility in the choice of tools for researchers and practitioners.

While EC has been a gold standard in the field, we have proved the viability of both BLS and SR, which particularly benefits from a significantly lower capital and operational

cost. Future work would benefit from offering practical recommendations for application scenarios and the viability of each technique at different operational point.

# APPENDIX

Figure 24 shows the scatter plots of the three systems after removing the time factor. The different sampling rates showed consistently satisficing correlation.

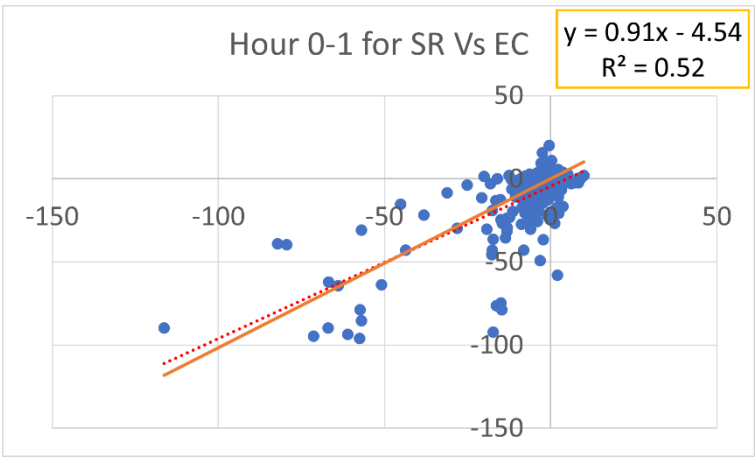


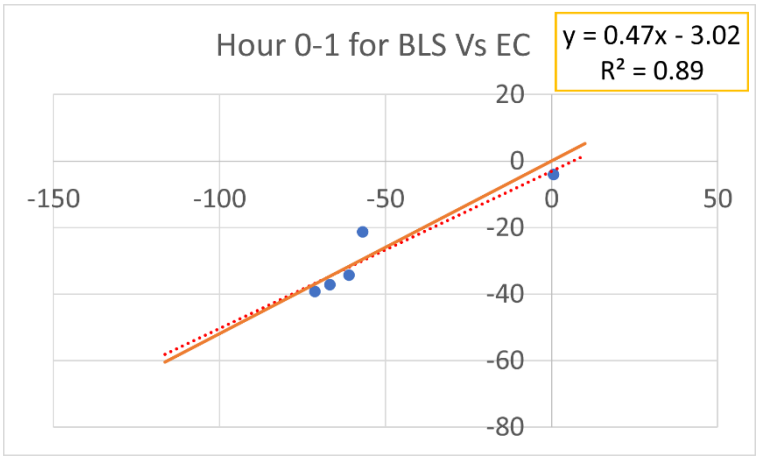


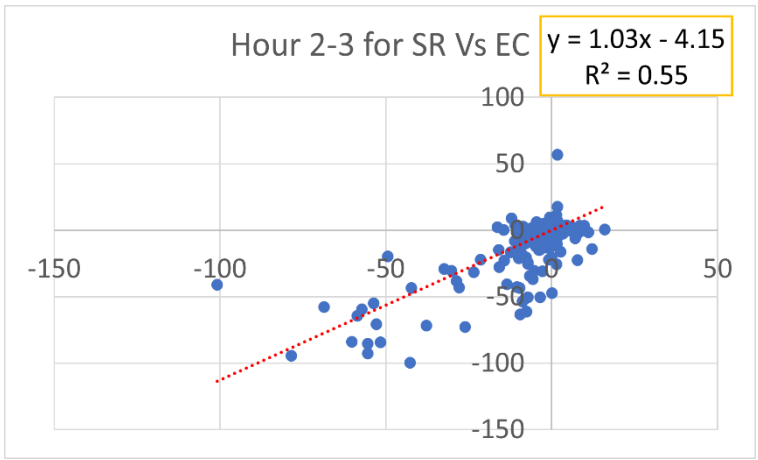


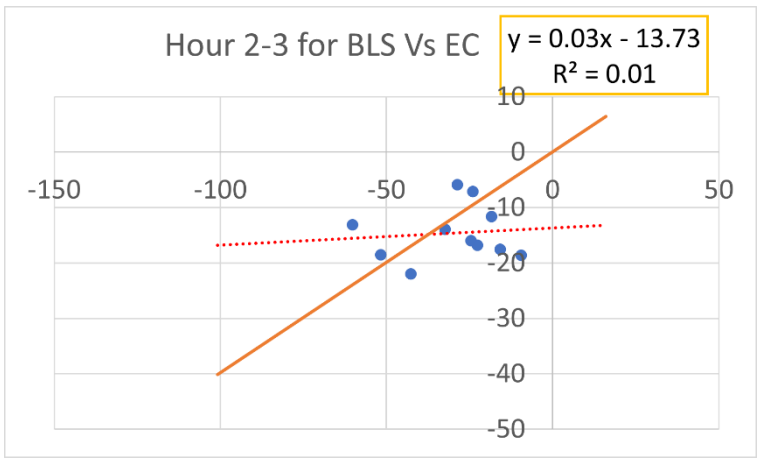


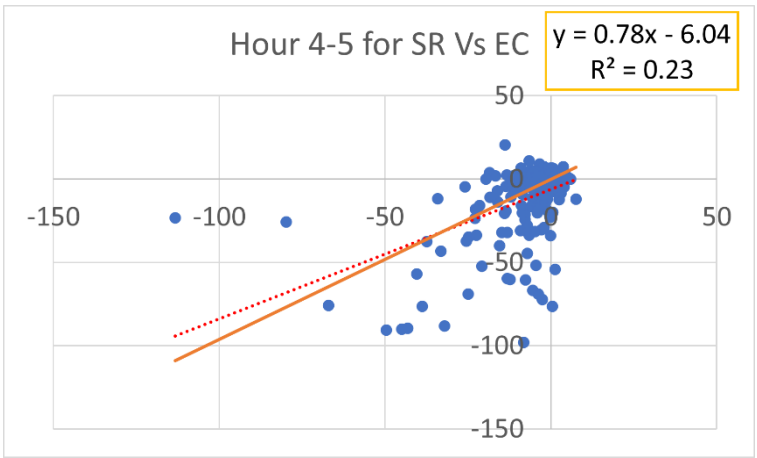


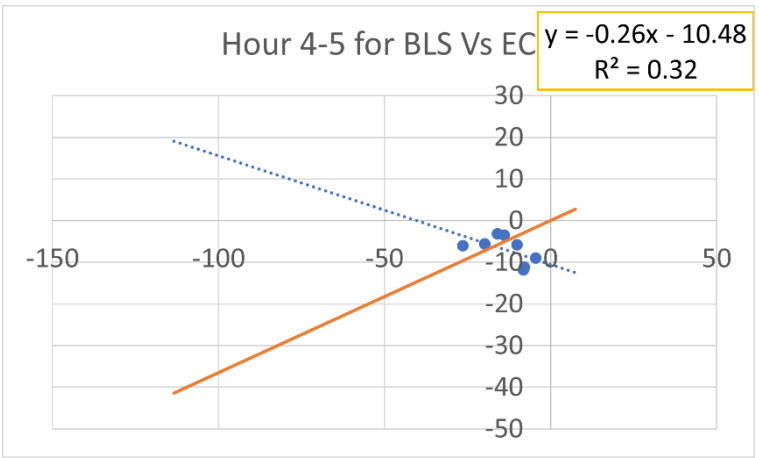

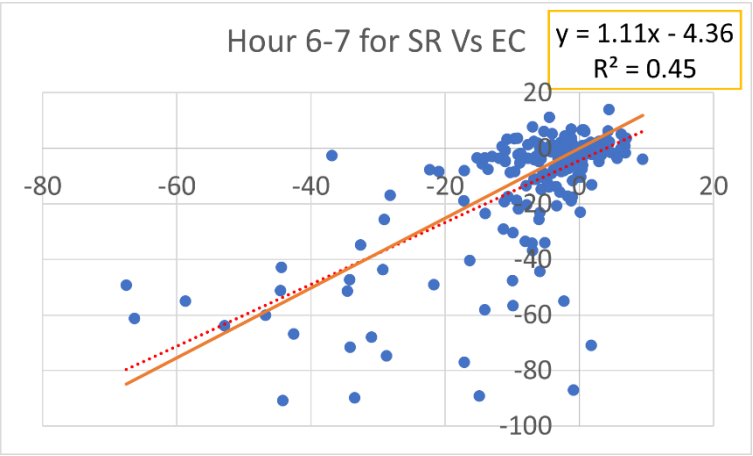
Hour 6-7 for SR Vs EC
y = 1.11x - 4.36
R² = 0.45

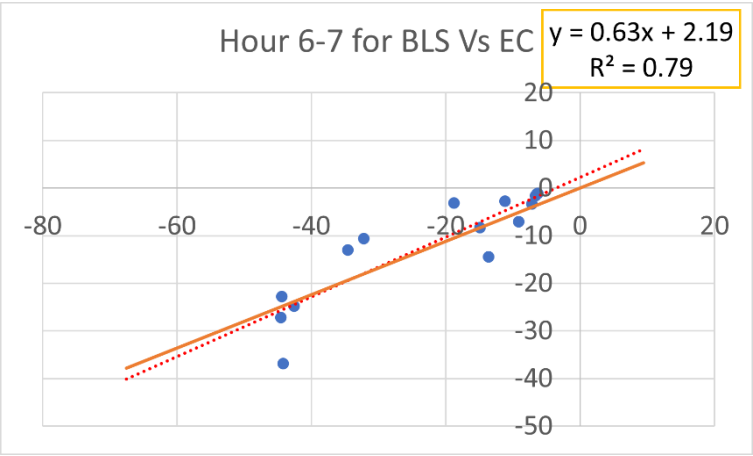
Hour 6-7 for BLS Vs EC
y = 0.63x + 2.19
R² = 0.79

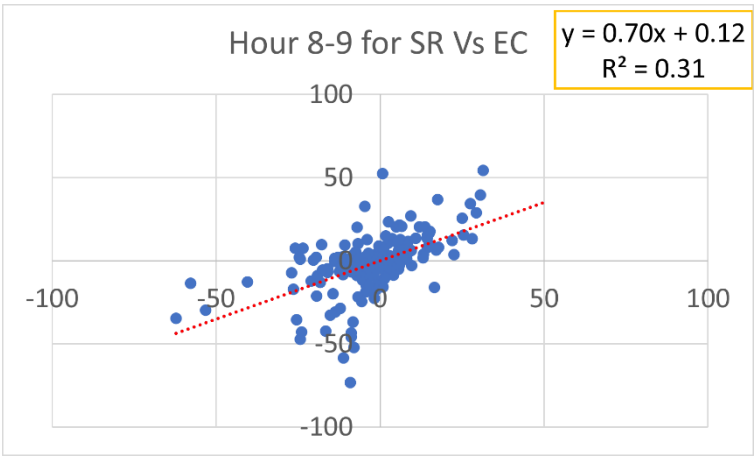
Hour 8-9 for SR Vs EC
y = 0.70x + 0.12
R² = 0.31

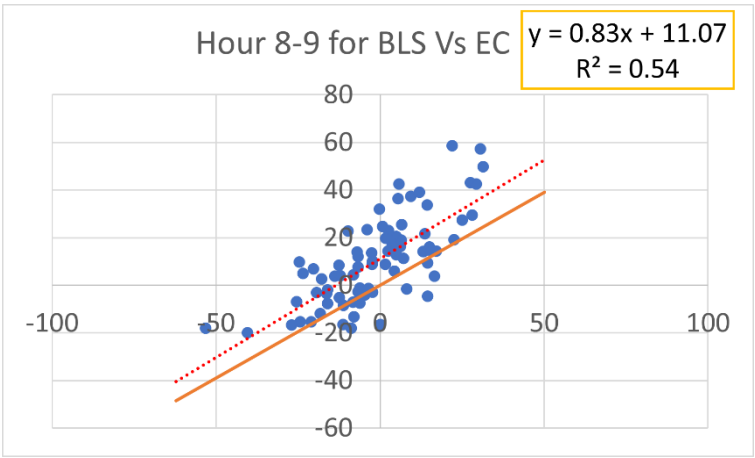
Hour 8-9 for BLS Vs EC
y = 0.83x + 11.07
R² = 0.54

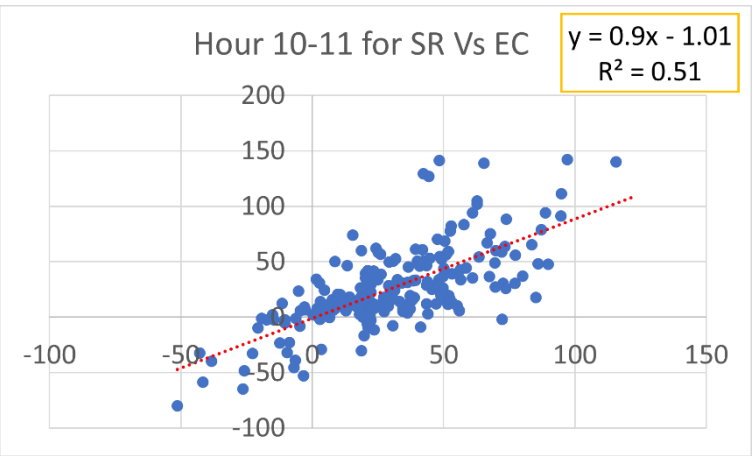
Hour 10-11 for SR Vs EC
y = 0.9x - 1.01
R² = 0.51

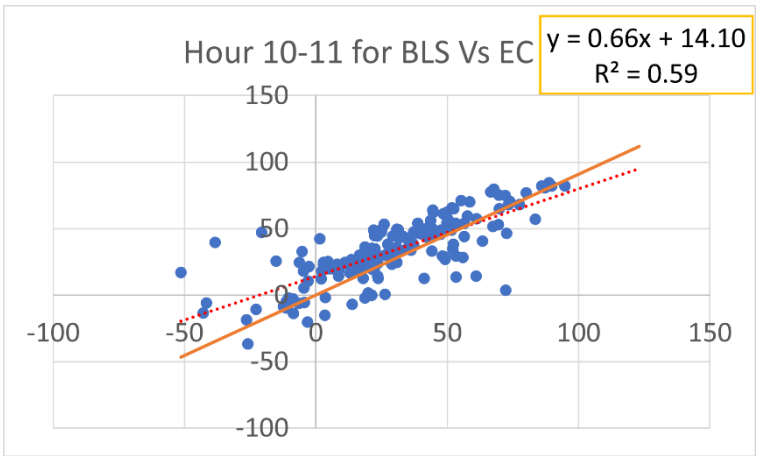
Hour 10-11 for BLS Vs EC
y = 0.66x + 14.10
R² = 0.59

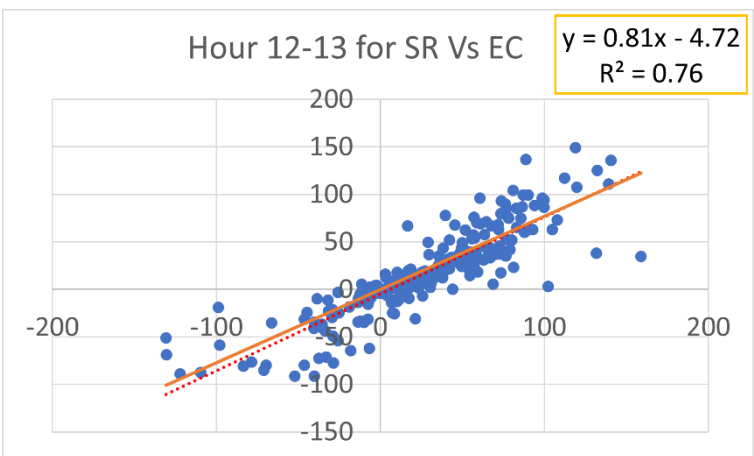
Hour 12-13 for SR Vs EC
y = 0.81x - 4.72
R² = 0.76

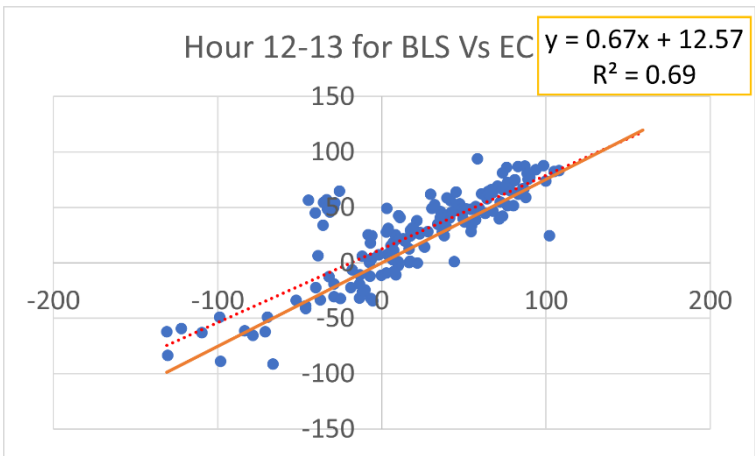
Hour 12-13 for BLS Vs EC
y = 0.67x + 12.57
R² = 0.69

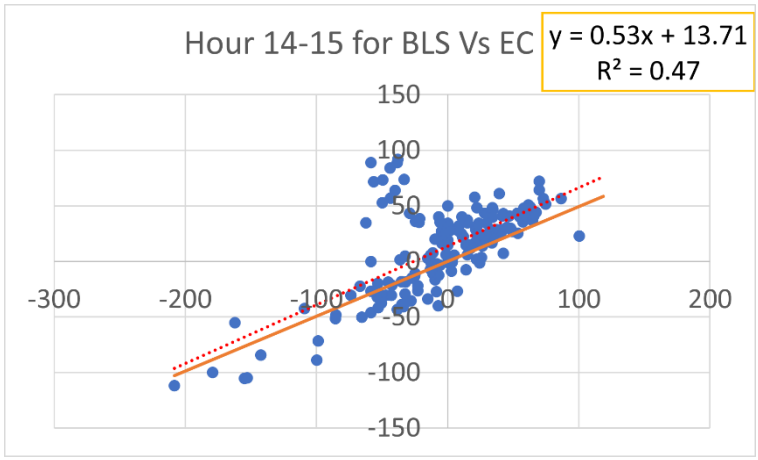
Hour 14-15 for BLS Vs EC
y = 0.53x + 13.71
R² = 0.47

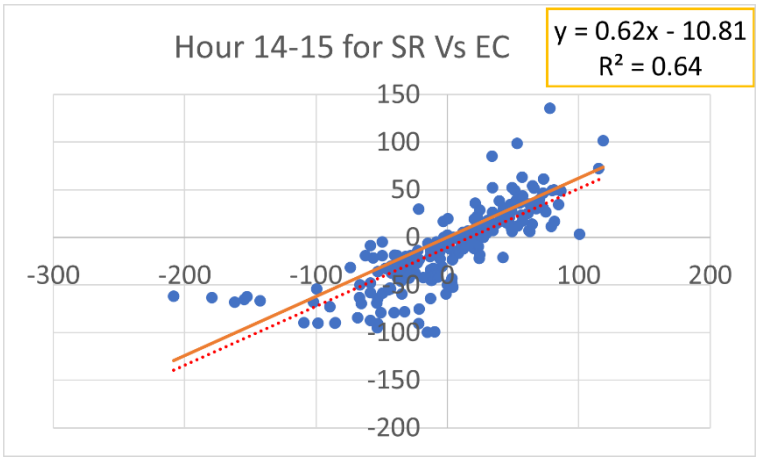
Hour 14-15 for SR Vs EC
y = 0.62x - 10.81
R² = 0.64

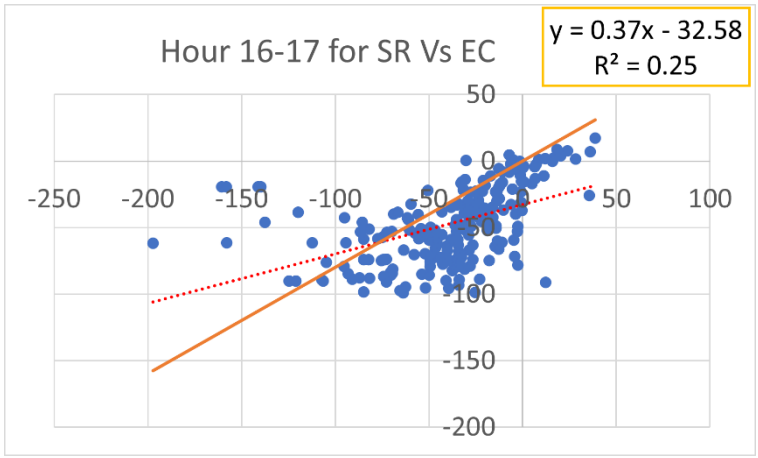
Hour 16-17 for SR Vs EC
y = 0.37x - 32.58
R² = 0.25

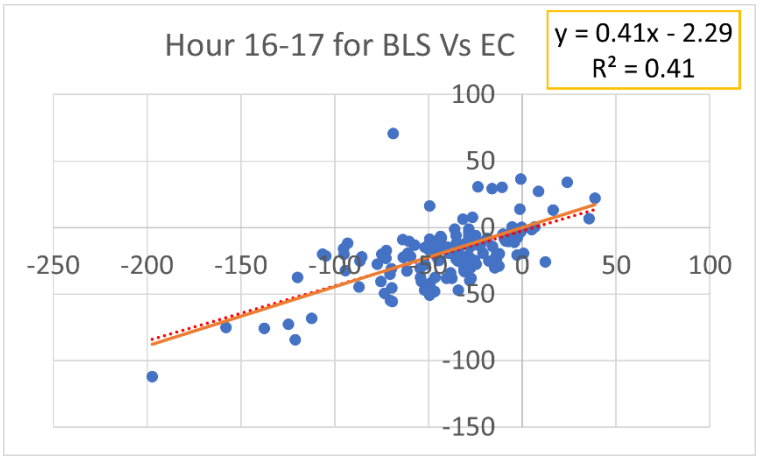
Hour 16-17 for BLS Vs EC
y = 0.41x - 2.29
R² = 0.41

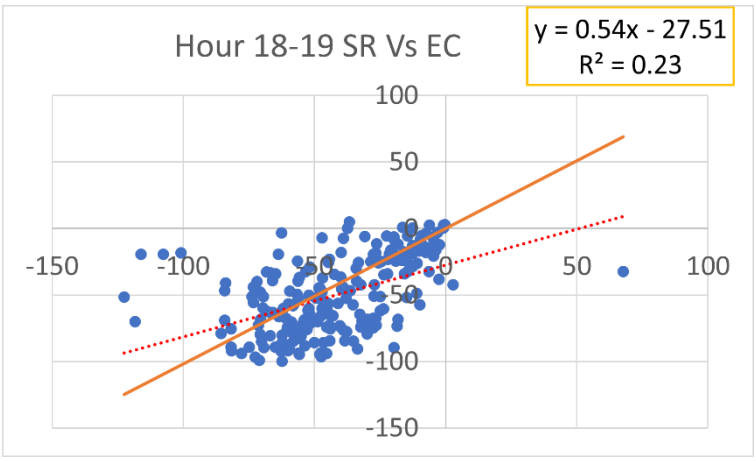
Hour 18-19 SR Vs EC
y = 0.54x - 27.51
R² = 0.23

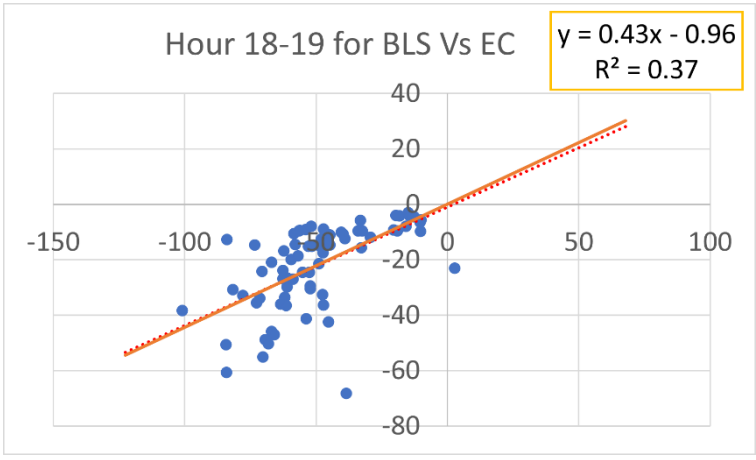
Hour 18-19 for BLS Vs EC
y = 0.43x - 0.96
R² = 0.37

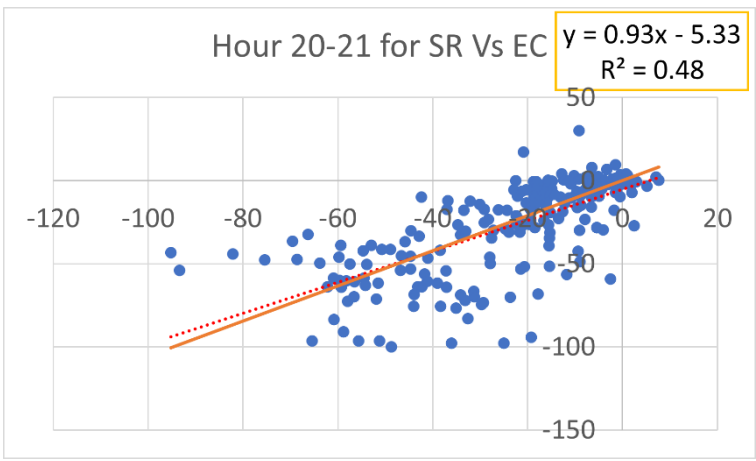
Hour 20-21 for SR Vs EC
y = 0.93x - 5.33
R² = 0.48

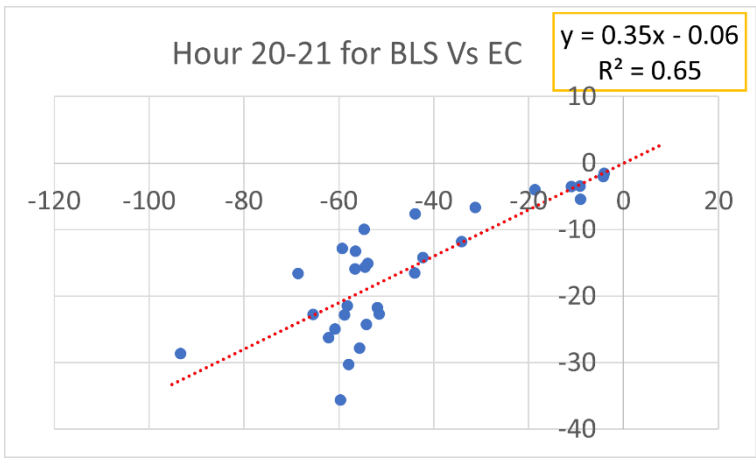
Hour 20-21 for BLS Vs EC
y = 0.35x - 0.06
R² = 0.65

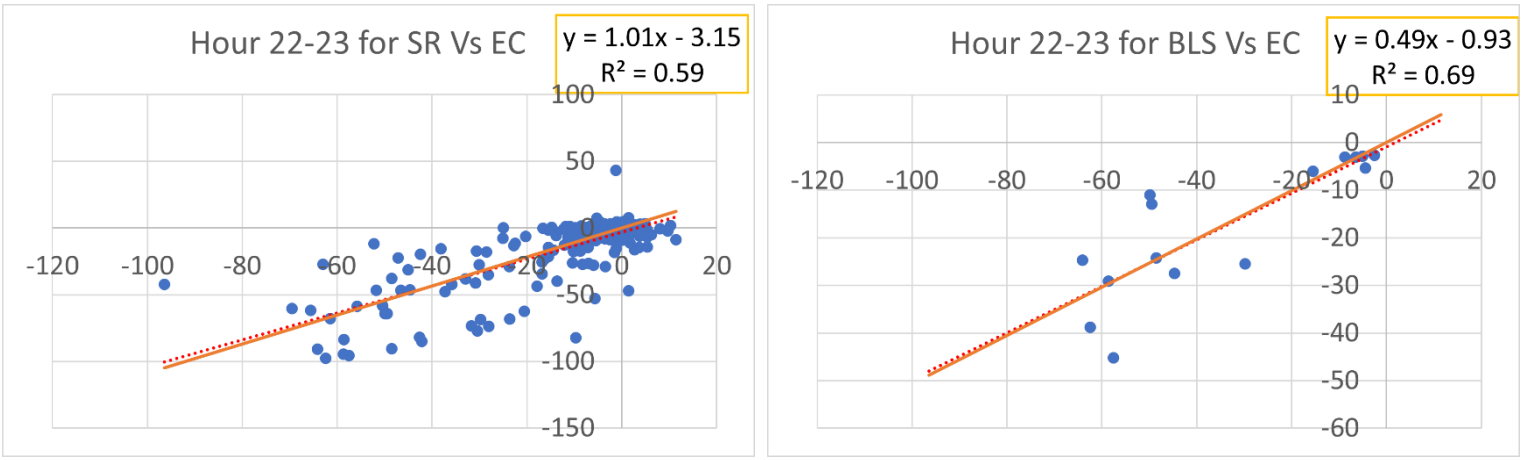


Figure 24 Scatter Plots after removing time dependent

# BIBLIOGRAPHY


Allen, R. G., Pereira, L. S., Howell, T. A., & Jensen, M. E. (2011). Evapotranspiration information reporting: I. Factors governing measurement accuracy. *Agricultural Water Management*, *98*(6), 899–920. https://doi.org/10.1016/j.agwat.2010.12.015

Asanuma, J., & Iemoto, K. (2007). Measurements of regional sensible heat flux over Mongolian grassland using large aperture scintillometer. *Journal of Hydrology*, *333*(1), 58–67. https://doi.org/10.1016/j.jhydrol.2006.07.031

Bambach, N., Kustas, W., Alfieri, J., Prueger, J., Hipps, L., McKee, L., Castro, S. J., Volk, J., Alsina, M. M., & McElrone, A. J. (2022). Evapotranspiration uncertainty at micrometeorological scales: The impact of the eddy covariance energy imbalance and correction methods. *Irrigation Science*, *40*(4–5), 445–461. https://doi.org/10.1007/s00271-022-00783-1

Beyrich, F., De Bruin, H. A. R., Meijninger, W. M. L., Schipper, J. W., & Lohse, H. (2002). Results from one-year continuous operation of a large aperture scintillometer over a heterogeneous land surface. *Boundary-Layer Meteorology*, *105*(1), 85–97. https://doi.org/10.1023/A:1019640014027

Braam, M., Bosveld, F. C., & Moene, A. F. (2012). On monin–obukhov scaling in and above the atmospheric surface layer: The complexities of elevated scintillometer measurements. *Boundary-Layer Meteorology*, *144*(2), 157–177. https://doi.org/10.1007/s10546-012-9716-7

Brunsell, N. A., Ham, J. M., & Arnold, K. A. (2011). Validating remotely sensed land surface fluxes in heterogeneous terrain with large aperture scintillometry. *International Journal of Remote Sensing*, *32*(21), 6295–6314. https://doi.org/10.1080/01431161.2010.508058

Campbell Scientific (2022a). CR1000X Measurement and Control Datalogger. Retrieved from https://www.campbellsci.com/cr1000x

Campbell Scientific (2022b). 18529 10 A 12 V Regulator with 15 ft Battery Cable. Retrieved from https://www.campbellsci.com/p18529

Campbell Scientific (2022c). FW3 Type E Fine-Wire Thermocouple with 0.003 in. Diameter. Retrieved from https://www.campbellsci.com/fw3

Campbell Scientific. (2022d). HygroVUE10 Digital Temperature and Relative Humidity Sensor with M12 Connector. Retrieved from https://www.campbellsci.com/hygrovue10

Campbell Scientific. (2022e). IRGASON Integrated CO2 and H2O Open-Path Gas Analyzer and 3-D Sonic Anemometer. Retrieved from https://www.campbellsci.com/irgason

Campbell Scientific. (2022f). TCAV-L Averaging Soil Thermocouple Probe. Retrieved from https://www.campbellsci.com/tcav-l

Campbell Scientific. (2022g). CS655 12 cm Soil Moisture and Temperature Sensor. Retrieved from https://www.campbellsci.com/cs655

Campbell Scientific. (2022h). HFP01-L Soil Heat Flux Plate. Retrieved from https://www.campbellsci.com/hfp01

Campbell Scientific. (2022i). NR01-L 4-Component Net Radiometer. Retrieved from https://www.campbellsci.com/nr01

Campbell Scientific. (2022j). HMP155A-L Air Temperature and Relative Humidity Sensor. Retrieved from https://www.campbellsci.com/hmp155a

Campbell Scientific. (2022k). CR6 Measurement and Control Datalogger. Retrieved from https://www.campbellsci.com/cr6

Campbell Scientific. (2022l). GRANITE VOLT 116 16- or 32-Channel 5V Analog Input Module. Retrieved from https://www.campbellsci.com/volt116

Castellvi, F., Martínez-Cob, A., & Pérez-Coveta, O. (2006). Estimating sensible and latent heat fluxes over rice using surface renewal. *Agricultural and Forest Meteorology*, *139*(1–2), 164–169. https://doi.org/10.1016/j.agrformet.2006.07.005

Castellví, F., Snyder, R. L., Baldocchi, D. D., & Martínez-Cob, A. (2006). A comparison of new and existing equations for estimating sensible heat flux using surface renewal and similarity concepts: ESTIMATING SENSIBLE HEAT FLUX. *Water Resources Research*, *42*(8). https://doi.org/10.1029/2005WR004642

Chicco, D., Warrens, M. J., & Jurman, G. (2021). The coefficient of determination R-squared is more informative than SMAPE, MAE, MAPE, MSE and RMSE in regression analysis evaluation. *PeerJ Computer Science*, *7*, e623.

Danodia, A., Sehgal, V. K., Patel, N. R., Dhakar, R., Mukherjee, J., Saha, S. K., & Kumar, A. S. (2017). Assessment of large aperture scintillometry for large-area surface energy fluxes over an irrigated cropland in north India. *Journal of Earth System Science*, *126*(5), 69. https://doi.org/10.1007/s12040-017-0847-6

Evans, J. G., McNeil, D. D., Finch, J. W., Murray, T., Harding, R. J., Ward, H. C., & Verhoef, A. (2012). Determination of turbulent heat fluxes using a large aperture scintillometer over undulating mixed agricultural terrain. *Agricultural and Forest Meteorology*, *166–167*, 221–233. https://doi.org/10.1016/j.agrformet.2012.07.010

Ezzahar, J., Chehbouni, A., Hoedjes, J. C. B., Er-Raki, S., Chehbouni, Ah., Boulet, G., Bonnefond, J.-M., & De Bruin, H. A. R. (2007). The use of the scintillation technique for monitoring seasonal water consumption of olive orchards in a semi-arid region. *Agricultural Water Management*, *89*(3), 173–184. https://doi.org/10.1016/j.agwat.2006.12.015

Geli, H. M. E., González-Piqueras, J., Neale, C. M. U., Balbontín, C., Campos, I., & Calera, A. (2019). Effects of surface heterogeneity due to drip irrigation on scintillometer estimates of sensible, latent heat fluxes and evapotranspiration over vineyards. *Water*, *12*(1), 81. https://doi.org/10.3390/w12010081

Gray, B. A., Toucher, M. L., Savage, M. J., & Clulow, A. D. (2021). The potential of surface renewal for determining sensible heat flux for indigenous vegetation for a first-order montane catchment. *Hydrological Sciences Journal*, *66*(6), 1015–1027. https://doi.org/10.1080/02626667.2021.1910268

Han, X., Zhou, Q., Zhang, B., & Xu, D. (2019). Research on variation rule of sensible heat flux in field under different soil moisture content and underlying surface by large aperture scintillometer. In D. Li (Ed.), *Computer and Computing Technologies in*

*Agriculture X* (Vol. 509, pp. 310–317). Springer International Publishing. https://doi.org/10.1007/978-3-030-06155-5_31

Hoedjes, J. C. B., Zuurbier, R. M., & Watts, C. J. (2002). Large aperture scintillometer used over a homogeneous irrigated area, partly affected by regional advection. *Boundary-Layer Meteorology*, *105*(1), 99–117. https://doi.org/10.1023/A:1019644420081

Hu, Y., Buttar, N. A., Tanny, J., Snyder, R. L., Savage, M. J., & Lakhiar, I. A. (2018). Surface renewal application for estimating evapotranspiration: A review. *Advances in Meteorology*, *2018*, 1–11. https://doi.org/10.1155/2018/1690714

Huang, M. fen, Liu, S. min, Guo, X., Zhu, Q., & Li, J. (2004). Analysis of the factors influencing surface sensible heat fluxes with large aperture scintillometers. *IGARSS 2004. 2004 IEEE International Geoscience and Remote Sensing Symposium*, *6*, 4281–4284 vol.6. https://doi.org/10.1109/IGARSS.2004.1370082

Kang, M., & Cho, S. (2021). Progress in water and energy flux studies in Asia: A review focused on eddy covariance measurements. 農業気象, *77*(1), 2–23. https://doi.org/10.2480/agrmet.D-20-00036

Kelley, J., & Higgins, C. (2018). Computational efficiency for the surface renewal method. *Atmospheric Measurement Techniques*, *11*(4), 2151–2158. https://doi.org/10.5194/amt-11-2151-2018

Keulertz, M. (2019). Water and Food Security Strategies in the MENA Region. MENARA Future Notes, (18).

Kleissl, J., Gomez, J., Hong, S.-H., Hendrickx, J. M. H., Rahn, T., & Defoor, W. L. (2008). Large aperture scintillometer intercomparison study. *Boundary-Layer Meteorology*, *128*(1), 133–150. https://doi.org/10.1007/s10546-008-9274-1

Liang, S., & Wang, J. (Eds.). (2020). Chapter 15 - Estimate of vegetation production of terrestrial ecosystem, Advanced remote sensing: terrestrial information extraction and applications (Second Edition). Academic Press, 581-620. https://doi.org/10.1016/B978-0-12-815826-5.00015-5

Liu, Y., Qiu, G., Zhang, H., Yang, Y., Zhang, Y., Wang, Q., Zhao, W., Jia, L., Ji, X., Xiong, Y., Yan, C., Ma, N., Han, S., & Cui, Y. (2022). Shifting from homogeneous to heterogeneous surfaces in estimating terrestrial evapotranspiration: Review and perspectives. *Science China Earth Sciences*, *65*(2), 197–214. https://doi.org/10.1007/s11430-020-9834-y

Liu, S. M., Xu, Z. W., Wang, W. Z., Jia, Z. Z., Zhu, M. J., Bai, J., & Wang, J. M. (2011). A comparison of eddy-covariance and large aperture scintillometer measurements with respect to the energy balance closure problem. *Hydrology and Earth System Sciences*, *15*(4), 1291–1306. https://doi.org/10.5194/hess-15-1291-2011

Li, X., Gao, Z., Li, Y., & Tong, B. (2017). Comparison of sensible heat fluxes measured by a large aperture scintillometer and eddy covariance system over a heterogeneous farmland in east china. *Atmosphere*, *8*(12), 101. https://doi.org/10.3390/atmos8060101

Morán, A., Ferreyra, R., Sellés, G., Salgado, E., Cáceres-Mella, A., & Poblete-Echeverría, C. (2020). Calibration of the surface renewal method (Sr) under different meteorological

conditions in an avocado orchard. *Agronomy*, *10*(5), 730. https://doi.org/10.3390/agronomy10050730

Parry, C. K., Shapland, T. M., Williams, L. E., Calderon-Orellana, A., Snyder, R. L., Paw U, K. T., & McElrone, A. J. (2019). Comparison of a stand-alone surface renewal method to weighing lysimetry and eddy covariance for determining vineyard evapotranspiration and vine water stress. *Irrigation Science*, *37*(6), 737–749. https://doi.org/10.1007/s00271-019-00626-6

Pozníková, G., Fischer, M., van Kesteren, B., Orság, M., Hlavinka, P., Žalud, Z., & Trnka, M. (2018). Quantifying turbulent energy fluxes and evapotranspiration in agricultural field conditions: A comparison of micrometeorological methods. *Agricultural Water Management*, *209*, 249–263. https://doi.org/10.1016/j.agwat.2018.07.041

Shock, C.C., Pereira, A.B.& Eldredge, E.P. Irrigation best management practices for potato. Amer J of Potato Res 84, 29-37 (2007)

Spano, D., Snyder, R. L., & Duce, P. (1997). Surface renewal analysis for sensible heat flux density using structure functions. Agricultural and Forest Meteorology, 86(3-4), 259-271.

Stagl, J., Mayr, E., Koch, H., Hattermann, F. F., & Huang, S. (2014). Effects of climate change on the hydrological cycle in Central and Eastern Europe. In Managing protected areas in central and eastern Europe under climate change (pp. 31-43). Springer, Dordrecht.

Vendrame, N., Tezza, L., & Pitacco, A. (2020). Comparison of sensible heat fluxes by large aperture scintillometry and eddy covariance over two contrasting−climate vineyards. *Agricultural and Forest Meteorology*, *288–289*, 108002. https://doi.org/10.1016/j.agrformet.2020.108002

Wang, J., Buttar, N. A., Hu, Y., Lakhiar, I. A., Javed, Q., & Shabbir, A. (2021). Estimation of sensible and latent heat fluxes using surface renewal method: Case study of a tea plantation. *Agronomy*, *11*(1), 179. https://doi.org/10.3390/agronomy11010179

Ward, H. C. (2017). Scintillometry in urban and complex environments: A review. *Measurement Science and Technology*, *28*(6), 064005. https://doi.org/10.1088/1361-6501/aa5e85

Wever, L. A., Flanagan, L. B., & Carlson, P. J. (2002). Seasonal and interannual variation in evapotranspiration, energy balance and surface conductance in a northern temperate grassland. Agricultural and Forest meteorology, 112(1), 31-49. https://doi.org/10.1016/S0168-1923(02)00041-2

Zhao, J., Olivas, P. C., Kunwor, S., Malone, S. L., Staudhammer, C. L., Starr, G., & Oberbauer, S. F. (2018). Comparison of sensible heat flux measured by large aperture scintillometer and eddy covariance in a seasonally-inundated wetland. *Agricultural and Forest Meteorology*, *259*, 345–354. https://doi.org/10.1016/j.agrformet.2018.05.026